Muscle-tendon unit properties in mice bred for high levels of voluntary running: novel physiologies, coadaptation, trade-offs, and multiple solutions in the evolution of endurance running

Alberto A. Castro[1], Allyn Nguyen[1], Saad Ahmed[1], Theodore Garland, Jr. [1], Natalie C. Holt[1]*

[1]Department of Evolution, Ecology and Organismal Biology, UC Riverside, Riverside, CA

*Corresponding author

Running page head: Adaptation of the muscle-tendon unit for endurance running

Keywords: artificial selection, locomotion, speed, running economy, cost of transport

Acknowledgements

This work was funded by NSF grant IOS-2038528 to T.G. and N.C.H. We thank other members of the Garland lab for helping to obtain the animals used here.

What is already known: Coadaptation, trade-offs and multiple solutions are known to complicate our understanding of relationship between underlying traits, performance, and fitness. Changes to muscle morphology, muscle physiology and tendon stiffness have been correlated with endurance running performance, variable evidence for trade-offs between muscle speed and endurance has been presented, and novel physiologies that circumvent this trade-off have been reported.

What this study adds: This study leverages an artificial selection experiment to directly demonstrate adaptation in muscle and tendon properties for endurance running and allow for the exploration of coadaptation, trade-offs and multiple solutions. We show that selection results in longer tendons and shorter muscles and has variable effects on muscle speed and endurance. These results provide the first direct evidence for the evolution of long distal tendons as an adaptation for endurance running, suggest a novel coadaptation of muscle and tendon properties, show that there are multiple combinations of muscle subordinate traits that increase endurance performance, and highlight that selection results in a speed-endurance trade-off that can sometimes be circumvented by novel physiologies.

Abstract

Muscle-tendon unit (MTU) morphology and physiology are likely major determinants of locomotor performance, and therefore Darwinian fitness. However, the relationships between underlying traits, performance, and fitness are complicated by phenomena such as coadaptation, multiple solutions, and trade-offs. Here we leverage a long-running artificial selection experiment in which mice have been selected for high levels of voluntary running to explore MTU adaptation, and the role of coadaptation, multiple solutions, and trade-offs, in the evolution of endurance running. We compared the morphological and contractile properties of a major locomotor MTU, the triceps surae complex, in 4 replicate selected lines to those in 4 replicate control lines. All selected lines have lighter and shorter muscles, longer tendons, and faster muscle twitch times than all control lines. Absolute and normalized maximum muscle shortening velocities, and contractile endurance, vary across selected lines. Absolute velocities are similar or lower, and endurance higher, in selected than control lines. However, normalized shortening velocities are both higher and lower in selected than control lines. These findings potentially show an interesting co-adaption between muscle and tendon morphology and muscle physiology, highlight multiple solutions for increasing endurance running performance, demonstrate that a trade-off between muscle speed and endurance can arise in response to selection, and suggest that a novel physiology may sometimes allow this trade-off to be circumvented.

Introduction

Skeletal geometry (Jenkins and Camazine 1977; Garland and Janis 1993), muscle morphology (Foster and Lucia 2007; Rubenson et al. 2011) and physiology (Gleeson and Harrison 1988; Rivero et al. 1993; Bonine et al. 2005), and tendon properties (Alexander et al. 1979; Pollock and Shadwick 1994; Arampatzis 2006) are major determinants of locomotor performance abilities, and therefore Darwinian fitness (e.g., escaping predators, foraging for food/territories) (Lappin and Husak 2005; Husak 2006). Understanding these relationships between underlying (subordinate) traits, organismal performance, and fitness is a primary goal of evolutionary physiology (Bartholomew 1964; Arnold 1983; Garland and Carter 1994). However, these relationships are complicated by phenomena such as coadaptation, where coordinated changes in multiple traits are required for increased performance (Mayr 1963; Huey and Bennett 1987; Foster et al. 2018); multiple solutions, where more than one combination of trait values can result in the same level of performance (Garland 2003; Wainwright et al. 2005; Garland et al. 2011; Moen 2019); and trade-offs, where increases in one facet of performance necessarily decrease another (Lindstedt et al. 1998; Wilson et al. 2002; Castro et al., 2022; Garland et al. 2022). For example, among species of skinks, fore and hindlimb lengths are coadapted in a way that appears to facilitate climbing behavior (Foster et al. 2018), several combinations of hindlimb bone lengths and muscle masses result in the same jump performance across frog ecomorphs (Moen 2019), and space constraints in skeletal muscle fibers means that volume allocated to the calcium stores required for high frequency contractions trades off against that allocated to the contractile proteins required for high power outputs (Lindstedt et al. 1998). Here, we examine adaptation in a major locomotor muscle-tendon unit (MTU) in response to artificial selection for endurance running in mice. Our results provide interesting examples of coadaptation, multiple solutions, and trade-offs.

The muscle-tendon unit is a highly organized, multi-scale, structure (Williams and Holt 2018; Holt 2019). Contractile protein filaments, actin and myosin, are arranged into sarcomeres. These sarcomeres are then organized in series along myofibrils and packaged in parallel, along with calcium stores and metabolic enzymes, into muscle cells or fibers. Muscle fibers are organized with a parallel or pennate geometry to form the muscle belly, which is then connected to the skeleton via aponeuroses and a tendon. Muscle consumes metabolic energy to generate the mechanical output required for locomotion through the calcium-activated interactions between actin and myosin. Tendons transmit muscle output to the skeleton and often store and return elastic strain energy.

Various aspects of muscle and tendon morphology and physiology determine muscle and locomotor performance. Potential for elastic strain energy storage is largely determined by tendon length and cross-sectional area (Pollock and Shadwick 1994; Ettema 1996; Holt and Mayfield 2023). Peak muscle force is determined by muscle cross-sectional area (CSA) and pennation angle (Powell et al. 1984; Wilson and Lichtwark 2011). Rate of muscle activation is determined by the calcium response, myosin isoform, and tendon elasticity (Hill 1951; Young and Josephson 1983; Rome et al. 1996; Lindstedt et al. 1998; Mayfield et al. 2016). Maximum muscle shortening velocity is determined by fiber length (Wilson and Lichtwark 2011) and myosin isoform (Schiaffino and Reggiani 2011). Metabolic energy consumption is determined by myosin isoform (He et al. 2000), muscle volume (Biewener and Roberts 2000), muscle shortening (Barclay 2023), and tendon elasticity (Roberts et al. 1997; Biewener and Roberts 2000; Holt et al. 2014). Finally, endurance is determined by the metabolic cost incurred (Hoogkamer et al. 2016; Fletcher and MacIntosh 2017) and the metabolic profile of muscle fibers (Rivero et al. 1999; Schiaffino and Reggiani 2011).

112 The relationships between underlying traits and muscle performance are relatively well understood.
113 However, they are neither simple nor independent. Locomotor performance is determined by the
114 interaction of many muscle and tendon properties; for example, strain energy storage in tendons
115 depends on the tight integration of muscle force and length change capacity and tendon stiffness
116 (Mendoza and Azizi 2021; Holt and Mayfield 2023). Many facets of performance are affected by
117 multiple underlying traits; for example, velocity may be increased both by increasing muscle fiber
118 length and the presence of a faster myosin isoform (Schiaffino and Reggiani 2011; Wilson and
119 Lichtwark 2011). These underlying traits do not always vary independently; for example, the
120 covariation of myosin isoform and metabolic enzymes results in stereotyped "fiber types," ranging
121 from slow fatigue resistant fibers to fast fatigable fibers (Rivero et al. 1999; Schiaffino and Reggiani
122 2011). Hence, adaptation in MTUs offers the opportunity to study a range of key phenomena in both
123 functional and evolutionary biology, including coadaptation, multiple solutions, and trade-offs.
124
125 Here we use the long-term "high runner" artificial selection experiment (Garland 2003; Garland and
126 Rose 2009) in which 4 replicate lines of high runner (HR) mice (lab designations HR3, HR6, HR7,
127 HR8) that have been bred for high levels of voluntary wheel running for nearly a hundred
128 generations are compared with 4 replicate control (C) lines (lab designations C1, C2, C4, C5) that
129 have been bred without regard to running (Swallow et al. 1998), to investigate adaptation for
130 endurance running in an MTU (Garland 2003; Houle-Leroy et al. 2003; Guderley et al. 2006;
131 Garland et al. 2011). This artificial selection approach allows for known, single-factor, selection and
132 so simplifies interpretation of evolutionary responses, and replicate lines allow for the identification
133 of multiple solutions and trade-offs.
134

The HR lines evolved rapidly and reached selection limits after ~17-27 generations (Careau et al. 2013), at which point mice from all 4 HR lines ran approximately three-fold more than those from the 4 C lines, largely due to an increase in speed (Girard et al. 2001; Garland et al. 2011). This increase in running distance is accompanied by changes in many underlying traits, including an increased maximal rate of oxygen consumption during forced exercise (VO_{2max}) and changes to running kinematics (Kolb et al. 2010; Claghorn et al. 2017; Schwartz et al. 2023). Most notably for this study, two lines of HR mice have evolved with the "mini-muscle" phenotype, a polymorphism caused by an autosomal recessive allele that appears to be under strong positive selection (Garland et al. 2002) and has reached fixation in HR3 (Garland et al. 2002; Syme et al. 2005) but remains polymorphic in HR6 (Hiramatsu et al. 2017). The mini-muscle phenotype results in a 50% loss of hindlimb muscle mass, a loss of fast type IIb muscle fibers, slower contractile properties, and altered efficiency of some muscles (Garland et al. 2002; Syme et al. 2005; Guderley et al. 2006; McGillivray et al. 2009; Talmadge et al. 2014). Hence, we distinguish between mini-muscle and normal-muscle mice and divide line HR6 into two groups (mini and normal) based on mini-muscle status (HR3M, HR6M, HR6N) and collectively distinguish between mini-muscle HR lines (HRmini) and normal-muscle HR lines (HRnorm). Variation in contractile speed and endurance, and trade-off between these, has previously been observed across the replicate lines of HR mice (Castro et al., 2022). Here we perform *in situ* muscle physiology experiments on the triceps surae (calf muscle) MTU, a distal limb muscle complex with a significant tendon that is a major contributor to locomotion, and compare its morphological and contractile properties across mice from all 4 HR and C lines to determine the effects of selection, and the potential for variation in the response to selection, on underlying traits.

158 Based on previous studies of increased endurance performance in individuals with exercise training,
159 across individuals in a population, and among species, we might expect several possible changes to
160 the MTU in response to the selection experienced by HR lines. Increased endurance performance,
161 and the increased running economy that often underpins it (Joyner and Coyle 2008; Hoogkamer et
162 al. 2016), has been associated with a decreased mass and length of distal limb muscles, increased
163 distal limb tendon length, and increased proportion of slower muscle fiber types. Reduced distal
164 limb muscle mass reduces limb swing costs (Myers and Steudel 1985; Rubenson et al. 2011).
165 Endurance training decreases muscle mass in humans (Trappe et al. 2006; Aagaard et al. 2011),
166 human populations with higher running economy have smaller distal limb muscles (Foster and Lucia
167 2007), and species assumed to be adapted for economical distance running have reduced distal limb
168 muscles (Alexander et al. 1979; Picasso 2010; Rubenson et al. 2011). Increased tendon length allows
169 for greater storage and return of elastic strain energy during running, which can reduce muscle work
170 during running and allow for short muscles that produce force cheaply (Pollock and Shadwick 1994;
171 Ettema 1996; Roberts et al. 1997; Holt et al. 2014; Labonte and Holt 2022; Holt and Mayfield 2023).
172 Increased potential for elastic strain energy storage with training improves running economy in
173 humans (Arampatzis 2006; Fletcher and MacIntosh 2017) and, across a diverse range of taxa,
174 species presumed to be adapted for economical distance running often have shorter muscle fibers
175 and longer tendons in distal MTUs (Alexander et al. 1979; Alexander 1991; Pollock and Shadwick
176 1994; Biewener and Roberts 2000; Picasso 2010; Rubenson et al. 2011). An increased proportion
177 of slower, oxidative fibers reduces metabolic cost and confers fatigue resistance. Endurance training
178 increases the proportion of slower fiber types in humans (Andersen and Henriksson 1977) and
179 muscle oxidative enzymes in rodents (Green et al. 1983; Houle-Leroy et al. 2000), competitive
180 endurance horses with excellent performance records have a higher proportion of oxidative fiber

types than less successful individuals (Rivero et al. 1993) and higher levels of oxidative enzymes correlate with endurance capacity among individual lizards within a single lizard species (Garland and Else 1987). Among species of lizards, variation in muscle fiber type appears to explain some of the variation in running endurance (Bonine et al. 2005; Albuquerque et al. 2015; Scales and Butler 2016), and selection for endurance running increase oxidative metabolic enzyme activity (Houle-Leroy et al. 2000). Considering these various lines of evidence from both human and non-human vertebrates, we predicted that mice from HR lines would have smaller muscles and longer tendons than those from C lines, and that their muscles would be slower and have higher endurance, reflecting a shift in fiber type composition towards a slower, more oxidative fiber type. However, given the required integration between traits, the many traits affecting performance, and the stereotyped covariation of aspects of muscle fibers, we also expected to observe coadaptation between tissues, multiple solutions that enable increased endurance running performance, and trade-offs between speed and endurance.

It should be noted that a subset of these data, the contractile properties of HR lines, have been published previously, and a trade-off demonstrated between contractile speed and endurance across the replicate HR lines (Castro et al. 2022). However, the inclusion of morphological data and unselected C lines in the present study expands on this published data by allowing us to directly test the effects of selection on MTU morphological and contractile properties, to examine the effects of selection on the coadaption of muscle and tendon, and to explore whether the observed trade-offs and multiple solutions arise only in response to selection.

Methods

The morphological and *in situ* contractile properties of the triceps surae MTU of HR and C mice were quantified. The triceps sure MTU is composed of 4 muscles: the soleus, plantaris and medial and lateral gastrocnemii. These muscles originate from the femur and the tibia (soleus) and insert onto the calcaneus via long tendons, most notably the large Achilles tendon (Charles et al., 2016). Isometric twitch and tetanic contractions, isotonic shortening contractions, and repeated isometric tetanic contractions were performed, and muscle belly length, tendon length, whole MTU length, muscle complex mass, and body mass were measured. This study of the entire triceps surae MTU *in situ* provides the best estimates of muscle performance in the context of locomotion as it allows for the determination of the emergent properties of these synergistic muscles while connected to a functioning circulatory system. These factors are particularly crucial in the HR mouse system and for the questions to be addressed here as selection has previously been demonstrated to have different effects on the various muscles in the triceps surae complex (Houle-Leroy et al. 2003; Syme et al. 2005; Castro et al., 2022), and measurements of endurance are complicated by diffusion limitations in *in vitro* preparations where the muscle is isolated from the circulatory system (Barclay 2005; Castro et al., 2022).

Study animals

The founding population of the HR model consisted of 224 laboratory house mice (*Mus domesticus*) of the outbred, genetically variable Hsd:ICR strain (Harlan-Sprague-Dawley, Indianapolis, Indiana, USA). Mice were randomly bred for two generations and then separated into 8 closed lines, 4 HR (HR3, HR6, HR7, and HR8) and 4 C (C1, C2, C4, and C5). Each line contained 10 breeding pairs. Since then, each generation of mice are weaned at 21 days old and housed in same-sex groups of 4 until 6-8 weeks old. Mice are then housed individually in their respective home cage with a

computer-monitored wheel for 6 days. In the HR lines, the highest-running male and female from each family are chosen as breeders. In control lines, breeders are chosen without regard to their running ability (sibling mating is not allowed) (Swallow et al. 1998; Careau et al. 2013; Hiramatsu et al. 2017; Cadney et al. 2021).

For this experiment, female mice from generations 91 (HR; N=31) and 94 (C; N=23) of the selection experiment were used. Due to the large number of mice and surgical nature of the experiment, it was not possible to complete all measurements within a single generation. Hence, C and HR mice are from different generations, and some variation in age occurred within generations (mice ranged from 46-171 days old). For graphing and statistical analyses, line HR6 was split into 2 (HR6N and HR6M) and line 3 designated as HR3M to indicate the presence of the mini-muscle phenotype. All HR3 mice, and 6/13 HR6 mice had the mini-muscle phenotype. The latter were assigned to the HR6M group. Sample sizes for each of the C lines were 7, 6, 6 and 4 for C1, C2, C4 and C5, respectively, and for the HR lines they were 6, 5, 6, 8 and 6 for HR3M, HR6M, HR6, HR7 and HR8, respectively. Mice were housed at room temperature with food and water ad libitum, 4 per cage, beginning at weaning. All experiments were approved by the University of California, Riverside Institutional Animal Care and Use Committee.

In situ muscle preparation

Mice were anaesthetized (SomnoSuite Low-flow Anesthesia System, Kent Scientific, Torrington, CT, USA), and an adequate plane of anesthesia maintained throughout the experiment. The sciatic nerve was surgically exposed, and a bipolar nerve cuff placed around it to allow for electrical stimulation of the triceps surae muscle complex. The proximal end of the femur was exposed and

clamped into a custom-made stereotaxic frame. The distal portion of the MTU was exposed and the calcaneus cut, tied with inextensible Kevlar thread, and connected to the lever arm of a servomotor (305C-LR Dual-Mode Lever System, Aurora Scientific, Aurora, ON, CA) to allow for measurements of MTU force and length (Holt et al. 2016).

Muscle contractions were elicited using supramaximal square wave pulses of amplitude 1-2 mA and pulse duration 0.1 ms (IgorPro 7, WaveMetric, Lake Oswego, OR, US; CompactDAQ, National Instruments, Austin, TX, US; High-Power, Biphase Stimulator, Aurora Scientific, Aurora, ON, CA). Stimulus pulses were delivered and MTU force and length data logged at 10,000 Hz (IgorPro 7, WaveMetric, Lake Oswego, OR, US; CompactDAQ, National Instruments, Austin, TX, US). Single stimulus pulses were used to elicit twitch contractions at a range of lengths. The length yielding maximum twitch force was designated as optimum length (L_0), and all subsequent contractions were performed, and morphological measurements made, at this length. An additional twitch contraction was performed at optimum length to allow for determination of force rise and relaxation times. Repeated stimulus pulses were applied at 80 Hz for 350ms to elicit an isometric tetanic contraction from which peak isometric force (corrected for passive force) could be determined. This isometric contraction was repeated at ~3 contraction intervals to monitor muscle performance. If force had dropped below 90% of its initial value by the first control isometric tetani, the experiment was terminated as it was assumed that the muscle or nerve had been damaged during surgery. The experiment continued if force dropped after this point to avoid biasing our sample against muscles with low endurance.

Isotonic tetanic contractions were performed at a range of relative forces (0.1-0.9 F_0), and the muscle-tendon complex allowed to shorten to maintain these forces. Force produced and peak shortening velocity were determined at each of these force levels. For each muscle, we performed 13 total contractions, including isotonic shortening contractions and isometric controls. The MTU was given 4 minutes rest between each contraction to allow for recovery. Following these isolated isometric and isotonic contractions, repeated isometric tetanic contractions (one contraction every 5 secs) were performed until force dropped below 50% of its initial value, or for a maximum of 500 contractions (whichever came first), to allow for determination of endurance. Following completion of the endurance protocol, an overdose of isoflurane anesthesia was administered and the triceps surae MTU fully exposed. The lengths of the Achilles tendon (the start of the common tendon proximally to the calcaneus distally), triceps surae muscle belly (muscle origin on the femur proximally to the start of the common Achilles tendon distally), and entire triceps surae MTU (muscle origin on the femur proximally to the calcaneus distally) were measured while the mouse was still in the stereotaxic frame and the MTU was at L_0. Mice were then removed from the frame and decapitated. The triceps surae muscle-tendon complex was dissected out and body and muscle belly mass determined. Muscle fiber lengths for the individual muscles in the triceps surae complex were not measured. A shorter muscle belly length is likely indicative of a shorter muscle fiber length (Powell et al., 1984). However, in pennate muscles such as those used here (Charles et al., 2016), muscle belly length is likely also affected by pennation angle.

Data analysis

Peak muscle force (F_0) was determined as the peak force produced during a maximum isometric tetanic contraction. A measurement of muscle cross-sectional area (CSA; not accounting for

295 pennation angle or fiber length as these are unknown) was determined from muscle mass and length
296 assuming a density of 1.06 kg/m^3 (Mendez and Keys, 1960). A metric of peak tetanic stress (σ_0)
297 was calculated as peak force normalized to cross-sectional areas ($\sigma_0 = F_0/CSA$). Twitch time series
298 data were used to calculate the time from onset of muscle activation to peak twitch force (TP_{tw}) and
299 time from peak twitch force to 50% relaxation (TR_{50}). Tetanic isotonic time series data was used to
300 determine force (F) and peak shortening velocity (V) during each contraction. Force-velocity curves
301 were constructed for each mouse, the data were fit with a second-order polynomials (see Castro et
302 al. 2022 for Marsh-Bennet and Hill curve-fits): $V = Ax^2+Bx+C$ (Castro et al. 2022) and maximum
303 shortening velocity (V_{max}) was calculated. Force was normalized by peak isometric force (F/F_0),
304 velocity was normalized by muscle belly length (V_{norm}) and maximum normalized shortening
305 velocity ($V_{normmax}$) was determined. This use of muscle belly length rather than fiber length should
306 be noted as, although these are likely to be related, muscle belly length does not directly reflect the
307 number of sarcomeres in series. For the endurance protocol, peak force was determined in every
308 contraction and plotted against contraction number (~200-500 contractions). Endurance was
309 quantified as the linear fit (slope) of the decline in force over the first 90 tetanic contractions ($Endur_{0-90}$)
310 and the force that could be sustained over a series of tetanic contractions was determined and
311 normalized to peak isometric tetanic force (Sustained F/F_0) (Castro et al. 2022).
312
313 *Statistical Analysis*
314 The Mixed procedure in SAS (SAS Institute, Cary, NC, USA) was used to analyze morphological
315 and isometric contractile properties (including endurance). Body mass and age were included as
316 covariates for morphological, but not contractile data (preliminary analyses revealed that the effect
317 of body mass was not significant). The effect of linetype (HR vs. C lines) included replicate line

318 nested within linetype as a random effect and was tested with 1 and 6 degrees of freedom. A main
319 effect of the mini-muscle phenotype (Garland et al. 2002; Houle-Leroy et al. 2003) was also
320 included and tested relative to the residual variance with 1 and ~43 d.f. (or fewer in the case of
321 missing values). In all analyses, outliers were removed when the standardized residual exceeded
322 ~3.0 and/or a value was >1 S.D. from the next residual, and we used an α of ≤ 0.05 for inferring
323 statistical significance. All of these analyses had a sample size of N=54 for each trait, except for
324 endurance metrics which had missing values (N=53 for $Endur_{0\text{-}90}$ and N=43 for Sustained F/F_0
325 respectively) and twitch time series data which had some high outliers (N=53 for TP_{tw} and N= 53
326 for TR_{50} respectively). The greater number of missing Sustained F/F_0 values is due to the experiment
327 occasionally being prematurely terminated before a constant force level was reached during early
328 experiments.
329
330 Given the nature of the force-velocity data points (Castro et al. 2022), we used repeated-measures
331 models in SAS Procedure Mixed to test for effects of linetype and the mini-muscle phenotype for
332 both V_{max} and $V_{normmax}$. Replicate line nested within linetype was a random effect, and the effect of
333 linetype was again tested with 1 and 6 degrees of freedom. The main effect of the mini-muscle
334 phenotype was again tested relative to the residual variance with 1 and ~351 d.f. (individual data
335 points). Covariates were age, relative force (F/F_0), and z-transformed relative force squared
336 (orthogonal polynomial). Furthermore, we included the interaction between force (F/F_0) and group
337 (F/F_o*line) to test for differences in slopes. Finally, we also included the interaction between
338 (Zfnorm2) and group (Zfnorm2*line) to test for differences in curvature in the F-V plots. Least
339 squares means generated from the repeated-measures analyses were calculated at $F/F_0 = 0$ to
340 estimate maximal shortening velocity from the 2nd degree polynomials for both absolute (V_{max}) and

normalized velocity ($V_{normmax}$). We used a formal outlier test (Cook and Sanford 1999) to make decisions about removing outliers (individual data points). For both absolute and normalized velocity, we removed all data from 4 mice due to poor force-velocity fits, one irregular data point with a normalized force of ~0.75 F_0 for one mouse, and all data from one mouse which was a high outlier for normalized velocity.

We also performed analyses that compared all eight lines, in addition to splitting line HR6 into two groups, one for mini-muscle individuals (HR6M) and the other for those with normal muscles (HR6N). We again used SAS Procedure Mixed, but "line" (N=9) was treated as a fixed effect. Covariates were as noted above. The nine "lines" were compared statistically using the differences of least squares means. We used the least squares means to make bar graphs and also to examine covariation of muscle performance metrics across the nine "lines" with bivariate scatterplots and pairwise Pearson correlation coefficients for σ_0, TP_{tw}, TR_{50}, V_{max}, $V_{normmax}$, $Endur_{0\text{-}90}$, and Sustained F/F_0. Correlations calculated separately for the five HR "lines" and for the four C lines were compared with a 2-tailed test in the cocor R package.

Results

Morphology

Body mass did not vary significantly with either linetype (HR vs C) ($p=0.5845$) or mini-muscle status ($p=0.2639$). However, with body mass as a covariate ($p<0.0001$), both linetype ($p=0.0027$) and mini-muscle status ($p<0.0001$) affected mass of the triceps surae complex; HR mice had lighter muscles than C mice, and mini-muscle mice had even lighter muscles (Fig. 1). Neither linetype ($p=0.1027$) nor mini-muscle status ($p=0.7161$) affected total MTU length (Fig. 1). However,

linetype affected both triceps surae muscle belly length ($p=0.0039$) and Achilles tendon lengths ($p=0.0016$); HR mice had significantly shorter muscle bellies and significantly longer tendons than C mice. This effect was consistent across all HR lines, with no effect of mini-muscle status on either muscle belly length ($p=0.7641$) or tendon length ($p=0.5935$) observed (Fig. 2, Supplemental Figure S1).

When comparing the nine "lines" (with line HR6 separated into HR6M and HR6N), with age as a covariate, body mass varied significantly ($p=0.0010$: Supplemental Figure S1 A) but did not show a differentiation among the groups of C, HRmini, and HRnorm (as reported in the previous paragraph). In addition to the linetype and mini-muscle effects noted in the previous paragraph (Fig. 1B), with body mass as a covariate, the mass of the triceps surae muscle complex varied among the three HRnorm lines (Supplemental Figure S1 B). Specifically, muscle mass was larger in HR8 than HR7 ($p=0.0114$), with values for HR6N being intermediate to them. In contrast, we did not detect differences among the four C lines. Total MTU length did not significantly vary among the nine "lines" ($p=0.0716$; Supplemental Figure S1 C) (with body mass as a covariate). However, with body mass as a covariate, muscle length varied among "lines" ($p<0.0001$: Supplemental Figure S1 A D). Specifically, line HR8 had longer muscles than either HR7 ($p=0.0488$) or HR6N ($p=0.0490$), but we did not detect statistically significant differences among the four C lines. Achilles tendon length did not vary significantly among either the five HR "lines" nor among the four C lines (Supplemental Figure S1 E).

Contractile properties

Peak isometric tetanic stress (σ_0) tended to be lower in HR than control mice (p=0.0726), with no effect of mini-muscle status (p=0.3075). Metrics of muscle speed were determined from the rates of force development and relaxation in isometric twitches and muscle shortening velocity during isotonic contractions. Metrics of muscle endurance were determined from the change in muscle force during repeated, tetanic, isometric contractions.

Speed

HR mice had significantly lower twitch rise times (TP_{tw}), indicating faster twitch rise times when compared with C mice (p=0.0286), with no significant effect of mini-muscle status (p=0.7016). Likewise, HR mice have significantly lower twitch half relaxation times (TR_{50}; p=0.0118), indicating faster relaxation, with no significant effect of mini-muscle status (p=0.4489) (Fig. 3).

Force-velocity data were plotted both as absolute (V_{max}; Fig. 4) and normalized ($V_{normmax;}$ Fig. 5) shortening velocities, with velocity normalized to muscle belly length in the latter. Data were fit with a second order polynomial as this provided the most consistent fit to the data, especially for HR lines (Castro et al. 2022). Linetype did not affect estimated V_{max} (p=0.3399), but mini-muscle individuals had lower values V_{max} than all other mice (p<<0.0001, Fig. 4A). We also found significant interactive effects of force and linetype (p<<0.0001) and of force and mini-muscle status (p<<0.0001) interactions (Fig. 4), indicating a difference in slope between HR and C and between mini-muscle and non-mini-muscle mice, and a $Zforce^2$ by linetype interaction effect (p<0.0001), indicating a difference in curvature between HR and C mice. When comparing the nine "lines" differences in V_{max} were apparent among the C lines, with C4 and C5 having higher values than C1

and C2 (pairwise $p<0.05$), and among the HRnorm lines, with HR8 having the highest values, HR7 the lowest, and HR6N intermediate (Fig. 4A, all pairwise $p<0.03$).

$V_{normmax}$ was affected by both linetype ($p= 0.0086$) and mini-muscle status ($p<<0.0001$). We also found significant force by linetype ($p<0.0001$) and force by mini-muscle status ($p<<0.0001$) effects (Fig. 5) indicating differences in slope between HR and C and between mini-muscle and non-mini mice, and a $Zforce^2$ by linetype effect ($p<<0.0001$), indicating a difference in curvature between HR and C mice. When comparing the nine "lines", $V_{normmax}$ was lowest in HRmini "lines" HR3M and HR6M, intermediate in all C lines and line HR7, and highest in HR6N and HR8 (Fig. 5A). Note that HR7 had significantly lower $V_{normmax}$ than either HR6N ($p=0.0003$) and HR8 ($p<0.0001$).

Endurance

Muscles from HR mice had significantly lower slopes of the decline in force over the first 90 contractions ($Endur_{0-90}$), indicating higher endurance, when compared with C mice ($p=0.0221$) and mini-muscle individuals had significantly lower $Endur_{0-90}$ values compared to normal-muscle mice ($p<<0.0001$) (Fig. 6). When comparing the nine "lines", significant variation was apparent among the four C lines and among the three HRnorm "lines" (Fig. 6A). Linetype did not have an overall effect on the relative level of force that could be sustained indefinitely (Sustained F/F_0) (Fig. 6B; $p=0.1901$). However, mini-muscle mice had much higher Sustained F/F_0 values than all other "lines", indicating higher endurance (Fig. 6B; $p<<0.0001$). Comparing the nine "lines" indicated no significant differences among the four C lines (all pairwise $p>0.23$), between the two mini-muscle lines ($p=0.33$) or among the three normal-muscle HR lines (all $p>0.13$).

Velocity-endurance correlations

Bivariate scatterplots and pairwise correlations of least squares means for the metrics of shortening velocity (V_{max}, $V_{normmax}$), endurance ($Endur_{0-90}$, Sustained F/F_0), and isometric contractile properties (σ_0, TP_{tw}, TR_{50}) are shown in Supplemental Figure S2. Correlations were calculated separately for the five HR "lines" and for the four C lines, then compared with a 2-tailed test in the cocor R package. For the five data points for the HR "lines," six correlations were statistically significant: V_{max} and $V_{normmax}$ (r=0.965, p=0.0077), V_{max} and $Endur_{0-90}$ (Fig. 7; r=-0.980, p=0.0033), V_{max} and Sustained F/F_0 (r=-0.927, p=0.0232), $V_{normmax}$ and $Endur_{0-90}$ (r=-0.983, p=0.0027), $V_{normmax}$ and Sustained F/F_0 (r=-0.954, p=0.0119), and $Endur_{0-90}$ and Sustained F/F_0 (r=0.974, p=0.0051). Across the four C lines, the only significant correlations were between V_{max} and stress (r=-0.954, p=0.0457) and TR_{50} and Sustained F/F_0 (r=0.996, p=0.0042). Significant differences between the HR and C correlations occurred for V_{max} and $Endur_{0-90}$ (p=0.0031), $V_{normmax}$ and $Endur_{0-90}$ (p=0.0019), and TR_{50} and Sustained F/F_0 (p=0.0417) with the former two indicating that selective breeding has resulted in the evolution of a trade-off between muscle velocity and endurance.

Discussion

Here we examine changes in a locomotor MTU in response to selective breeding for high endurance-running performance in order to better understand the relationship between muscle traits and locomotor behavior, and to explore the role of coadaptation, multiple solutions, and trade-offs in the relationships between underlying traits and performance (Mayr 1963; Bartholomew 1964; Arnold 1983; Huey and Bennett 1987; Garland and Carter 1994; Wainwright et al. 2005; Garland et al. 2011; Foster et al. 2018; Moen 2019). We compared the morphological and contractile properties of the triceps surae MTU in 4 lines of mice artificially selected for high levels of voluntary wheel-

running behavior to 4 control lines bred without regard for their running. Muscle mass, muscle belly length, and tendon length were determined as indicators of MTU morphology. Twitch rise (TP_{tw}) and half relaxation times (TR_{50}), absolute and normalized muscle force-velocity properties, and maximum shortening velocities ($V_{normmax}$ and V_{max}) were determined as indicators of muscle speed, and the slope of the initial decline in force ($Endur_{0\text{-}90}$) and the relative level of force that could be sustained indefinitely (Sustained F/F_0) were determined as metrics of muscle endurance. These metrics were determined for 7, 6, 6 and 4 mice for C1, C2, C4 and C5, respectively, and for 6, 5, 6, 8 and 6 mice for HR3M, HR6M, HR6, HR7 and HR8, respectively. Across this data set there were a small number of missing values or outliers that were removed. A single high outlier for TP_{tw} was removed from HR7 and for TR_{50} from C4. Absolute and normalized force-velocity curves had to be removed for 4 mice (HR6 (2), HR7, HR8) due to poor curve fits, likely due to the relatively low number of points used to characterize these curves to allow for subsequent reliable measurements of endurance. One outlier force-velocity point at ~0.75 F0 was removed for 1 mouse (C1), and 1 $V_{normmax}$ was removed due to being a high outlier (HR7). There were 2 missing values for $Endur_{0\text{-}90,}$ C2 and HR8, due to the mice dying under anesthesia before the endurance protocol could be completed and 11 missing values for Sustained F/F_0 (C1, C2, C4 (2), HR3M, HR6 (2), HR7, HR8 (3)) due to either the mice dying under anesthesia or the experiment being prematurely terminated before a sustained level of force was reached.

Morphology

Our results indicate that selection for voluntary wheel running has consistently favored a reduced muscle mass, a reduced muscle belly length -- which we interpret as some degree of reduction in muscle fiber length -- and an increased tendon length. All HR lines have lower muscle masses than

all C lines, and, within the HR lines, mice from HRmini lines have lower muscle masses than those from HRnorm lines (Fig. 1, Supplemental Figure S1). Total MTU length does not differ between HR and C lines (Fig. 1), but all HR lines have longer tendons and shorter muscle bellies than C lines (Fig. 2, Supplemental Figure S1). This reduction in muscle mass, and replacement of muscle belly length with tendon, will have reduced the mass of the distal limb in HR lines, and so presumably have reduced swing costs and/or allowed for faster swing (Myers and Steudel 1985; Rubenson et al. 2011; Labonte and Holt 2022) and more economical force generation during stance (Kram and Taylor 1990; Roberts et al. 1998; Beck et al. 2020). In addition to reduced distal limb mass, the longer tendons of HR mice likely also allow for greater storage and return of elastic strain energy during running (Pollock and Shadwick 1994; Ettema 1996; Biewener and Roberts 2000; Rubenson et al. 2011). This may have reduced the need for muscle fibers to do potentially costly work, and allowed for short muscle fibers that can produce the force required to support body weight cheaply (Roberts et al. 1997, 1998; Holt et al. 2014; Holt and Mayfield 2023).

The morphological changes in the triceps surae MTU in all HR lines in response to selection seem to suggest reduced locomotor costs, or increased running economy, which has been linked to increased endurance-running performance (Joyner and Coyle 2008; Hoogkamer et al. 2016). However, although a reduced total cost of locomotion has been observed in HR mice in previous generations (32 and 34), this effect was confounded by the smaller body masses of HR mice, resulting in no effect of selection on the mass-specific cost of transport (CoT) (Rezende et al. 2009). And at generation 46, CoT was found to be higher in mini-muscle than normal-muscle HR mice, mainly because of higher zero-speed intercepts in the regression of cost on running speed, and higher postural costs (Dlugosz et al. 2009). This lack of decrease, or even increase, in CoT with selection

for endurance running is surprising, given the changes to MTU morphology observed here (Figs. 1+2, Supplemental Figure S1). Other than decreased muscle mass and increased tendon length not conferring the widely assumed energetic benefits, we can propose several reasons for why this might be. Firstly, tendon length has not previously been examined in the HR mice, so we do not know if this adaptation had occurred when CoT was determined, or if it arose subsequently. Secondly, HR mice are smaller than C mice, and mass-specific CoT increases with decreasing body mass (Heglund et al. 1982). Hence, the similarity of mass-specific cost in HR and C lines may suggest adaptation for reduced cost in HR lines that offset this effect of size. Lastly, it may be that other changes counteract any savings due to reduced muscle mass and increase in tendon length, resulting in a constant CoT despite varying underlying traits. This latter point may relate to the question of whether small animals are able to use elastic tendons to achieve the same metabolic savings as large ones (Biewener et al. 1981; Bullimore and Burn 2005; Christensen et al. 2022). The evolution of long distal tendons in all 4 lines of HR mice shown here (Fig. 2) provides support for the benefits of long distal tendons for endurance running performance in small species (Bullimore and Burn 2005; Christensen et al. 2022). However, the lack of a reduced CoT (Rezende et al. 2009) suggests that they may not convey the same energetic benefits in small animals.

Contractile properties

Muscle twitch times and maximum shortening velocity were determined as metrics of muscle speed. All HR lines show faster twitch properties than C lines, indicating that selective breeding has increased the rate at which the muscle complex can be activated and deactivated (Fig. 3). This could be due to changes in calcium handling and sensitivity, myosin isoform, and/or tendon elasticity (Hill 1951; Young and Josephson 1983; Rome et al. 1996; Lindstedt et al. 1998; Mayfield et al. 2016).

However, the longer and presumably more compliant tendons in HR lines make it unlikely that faster twitch times are the result of increased tendon stiffness.

In general, absolute maximum shortening velocity is not different in HR than C lines. However, mini-muscle individuals have lower absolute maximum shortening velocity than other mice (Fig. 4) and absolute maximum shortening velocity varies across HR lines, including across HRnorm lines. Mini-muscle HR3M and HR6M had the lowest absolute velocities. Non-mini line HR8 had the highest and was comparable to C lines (Fig. 4). When absolute shortening velocity is normalized to muscle belly length, HRmini mice have the slowest normalized maximum shortening velocities, HRnorm lines HR6N and HR8 have the fastest, and all C lines plus HR7 are intermediate. This indicates that both faster and slower normalized maximum shortening velocities have evolved in response to selection (Fig. 5). Some caution should be taken with the interpretation of normalized shortening velocities due to normalization to muscle belly length rather than fiber length. However, assuming that reduced muscle belly length equates to shorter fibers, the similar or slower absolute, but faster normalized, maximum velocities seen in HRnorm lines HR6 and HR8 are likely the result of a combination of shorter muscles (Fig. 2) and faster myosin isoforms. The slower absolute and normalized maximum shortening velocities seen in mini-muscle HR mice are likely the result of shorter fibers and slower myosin isoforms (Bottinelli et al., 1994; Schiaffino and Reggiani 2011), the latter of which is consistent with the loss of the fast type IIb fibers previously observed in the mini-muscle phenotype (Guderley et al. 2006; McGillivray et al. 2009; Talmadge et al. 2014).

The faster normalized shortening velocities observed in some of the HRnorm lines are consistent with the faster twitch times seen in all HR lines (Fig. 3) and suggest that a faster myosin isoform

546 may contribute to both changes. However, the combination of slower normalized shortening
547 velocities and faster twitch times in HRmini lines is harder to explain, and potentially suggests a
548 faster calcium response and slower myosin isoform. This may support prior findings that indicate
549 that muscle speed can be increased in multiple, somewhat independent, ways (Anderson and Roberts
550 2020). The greatly reduced absolute velocity of HRmini lines (Fig. 4), due to shorter muscles
551 (Supplemental Figure S1) and slower myosin isoforms, likely explains the reduced sprint speed
552 observed in these lines (Dlugosz et al. 2009; Khan et al., 2024), and suggests that, while
553 physiologically feasible, this may not be a phenotype that is observed under natural, rather than
554 artificial, selection.
555
556 Rate of force decline and level of force that can be sustained were determined as metrics of muscle
557 endurance. All HR lines, and to a greater extent mini-muscle HR lines, have slower rates of force
558 decline and, in some cases, higher levels of sustained force than C lines (Fig. 6). This indicates that
559 selection has, to varying degrees, favored greater muscle endurance. This increased endurance is
560 likely due to a shift to a more economical muscle contraction and a more oxidative muscle fiber
561 type. The higher muscle endurance of HR lines (Fig. 6) likely enables their sustained faster wheel-
562 running running speeds (Lerman et al. 2002; Waters et al. 2008; Fletcher and MacIntosh 2017),
563 particularly in mini-muscle lines (Dlugosz et al. 2009; Garland et al. 2011), which are largely
564 responsible for the increased daily running distances (Girard et al. 2001; Garland et al. 2011).
565
566 *Coadaptation, multiple solutions, and trade-offs*
567 The relationship between underlying traits, performance, and fitness (reproductive success, which
568 in the HR lines is determined experimentally) is often complicated by the required coadaptation

between various traits (Mayr 1963; Huey and Bennett 1987; Bauwens et al. 1995; Foster et al. 2018), the potential for multiple solutions (Houle-Leroy et al. 2003; Wainwright et al. 2005; Garland et al. 2011; Moen 2019), and trade-offs between different aspects of performance (Lindstedt et al. 1998; Wilson et al. 2002; Garland et al. 2022). All the morphological and physiological changes to the MTU in response to selection reported here may be considered to be coadapted with the changes to locomotor behavior. However, we also observe what appears to be an interesting, and not previously described, coadaptation between muscle and tendon properties. All HR lines exhibit an increase in tendon length, and a concurrent decrease in muscle belly length (Fig. 2, Supplemental Figure S1). In some HRnorm lines, this appears to have been accompanied by an increase in normalized shortening velocity (Fig. 5), presumably due to a faster myosin isoform (Bottinelli et al., 1994; Schiaffino and Reggiani 2011). This increase in normalized velocity is counter to our predictions of slower, more oxidative fibers with higher endurance as the faster myosin isoforms likely responsible for faster normalized shortening velocities are typically accompanied by a more glycolytic metabolic profile (Rivero et al. 1999; Schiaffino and Reggiani 2011). We suggest this unexpected change in maximum normalized velocity might be a coadaptation with increased tendon, and reduced muscle belly, length. Reduced muscle length will have reduced absolute shortening velocity (Wilson and Lichtwark 2011), which is likely to have had disproportionate effect on locomotor performance in a small species (Kram and Taylor 1990; Labonte 2023). Hence, we suggest that potentially shifting to a faster myosin isoform may have allowed absolute muscle velocity to be maintained to some extent, despite shorter muscles. However, this change to a faster myosin isoform would likely offset some of the energy saving benefits of tendons (Barclay et al. 1993), and could explain the lower reliance on metabolic savings from long elastic tendons in small species (Biewener et al. 1981; Pollock and Shadwick 1994).

592

593 Multiple solutions are identified by different combinations of underlying traits that result in
594 approximately the same performance (Houle-Leroy et al. 2003; Wainwright et al. 2005; Garland et
595 al. 2011; Moen 2019). Although some of the underlying traits studied here, such as tendon length
596 and twitch time, change in similar ways across all HR lines, so indicating a single solution, we see
597 evidence of multiple solutions in muscle velocity and endurance. All HR lines run approximately
598 3x greater daily distances than C lines (Girard et al. 2001; Garland et al. 2011). However, selected
599 lines vary in absolute and normalized muscle shortening velocity and muscle endurance (Fig. 4-7).
600 These differences would arise from a combination of variance among populations at the onset of
601 selection and subsequent random genetic drift (Garland et al. 2002; Morgan et al. 2005) that changes
602 the genetic background within which genes and resultant phenotypes operate, thus potentially
603 constraining additional responses to selection.

604

605 We have previously described a trade-off between metrics of contractile speed and endurance across
606 the replicate HR lines (Castro et al., 2022). This finding supported the purported speed-endurance
607 trade-off in muscle functional properties (Garland, 1988; Wilson et al., 2002; and references
608 therein). However, the comparison with C lines presented here shows that although we see some
609 variation in muscle speed and endurance, as well as correlations between metrics of muscle
610 performance, across C lines, we do not see the negative correlation, and therefore evidence of a
611 trade-off, between metrics of muscle speed and endurance that we saw in the HR lines (Fig. 7;
612 Supplemental Figure S2). This indicates that, as expected, trade-offs may only be apparent under
613 strong selection when they limit the phenotypic space that can be occupied (Roff and Fairbairn 2007;
614 Shoval et al. 2012; Garland et al. 2022).

615

616 Trade-offs not only constrain phenotypic space but may also drive the evolution of novel
617 physiologies. For example, the frequency-power trade-off observed in muscle (Lindstedt et al. 1998)
618 has been circumvented by the evolution of asynchronous muscle in which calcium fluxes are no
619 longer directly linked to contraction (Josephson et al. 2000). We see some evidence of this in the
620 novel comparison of HR and C lines presented here, where mice from HR8 appear to have increased
621 muscle endurance compared to mice from C lines, with little to no reduction in absolute maximum
622 shortening velocity (Fig. 4+7) and an increase in normalized maximum shortening velocity (Fig. 5;
623 Supplemental Figure S2). We suggest that this may reflect a novel physiology, whereby a shift to
624 an oxidative, fatigue-resistant, fiber has not been accompanied by a shift to a slower myosin, so
625 disrupting the typical covariation of myosin isoform and metabolic enzymes that defines muscle
626 fiber types (Rivero et al. 1999; Schiaffino and Reggiani 2011). This is not unprecedented, as
627 locomotor muscles of several cursorial ungulates have high concentrations of both fast IIx myosin
628 and oxidative enzymes, suggesting fibers that are both fast and fatigue resistant (Kohn et al. 2011;
629 Curry et al. 2012; Kohn 2014)

630

631 **Conclusion**

632 Here we explore the effect of long-term selective breeding for high endurance-running performance
633 on the morphological and contractile properties of a distal limb MTU, the triceps surae complex,
634 across four replicate selected and four non-selected control lines of mice. Mice from selected (HR)
635 lines show reduced muscle mass and length, and an increase in tendon length, which likely reduces
636 the mass of the distal limb and increases elastic strain energy storage and return during running.
637 Mice from selected lines also have faster twitch times, similar or slower absolute shortening

velocities, both faster and slower normalized velocities (depending on the line) and higher contractile endurance. We document a combination of apparently faster normalized shortening velocities (presumably due to faster myosin isoforms), longer tendons, and shorter muscles that may represent coadaptation to somewhat maintain absolute contractile speed despite morphological changes. We identify various combinations of muscle speed and endurance across selected lines that all result in approximately the same increase in daily running distance, thus demonstrating multiple solutions. We show a trade-off between muscle speed and endurance that arises in response to selective breeding for endurance running, but also suggest that the faster muscles with higher endurance seen in a one HR line represents a combination of myosin isoform and metabolic properties that contrasts with our classic definitions of fiber types and so represents a novel physiology that circumvents this trade-off.

661 **Literature cited**

662 Aagaard P., J.L. Andersen, M. Bennekou, B. Larsson, J.L. Olesen, R. Crameri, S.P. Magnusson, et
663 al. 2011. Effects of resistance training on endurance capacity and muscle fiber composition in
664 young top-level cyclists: concurrent resistance and endurance training. Scand J Med Sci Sports
665 21:e298–e307.

666 Albuquerque R.L., K.E. Bonine, and T. Garland Jr. 2015. Speed and endurance do not trade off in
667 Phrynosomatid lizards. Physiol Biochem Zool 88:634–647.

668 Alexander R.McN. 1991. Energy-saving mechanisms in walking and running. J Exp Biol 160:55–
669 69.

670 Alexander R.McN., G.M.O. Maloiy, R. Njau, and A.S. Jayes. 1979. Mechanics of running of the
671 ostrich (*Struthio camelus*). J Zool 187:169–178.

672 Andersen P. and J. Henriksson. 1977. Training induced changes in the subgroups of human type II
673 skeletal muscle fibres. Acta Physiol Scand 99:123–125.

674 Anderson C.V. and T.J. Roberts. 2020. The need for speed: functional specializations of
675 locomotor and feeding muscles in *Anolis* lizards. J Exp Biol 223:jeb.213397.

676 Arampatzis A. 2006. Influence of the muscle-tendon unit's mechanical and morphological
677 properties on running economy. J Exp Biol 209:3345–3357.

678 Arnold S.J. 1983. Morphology, Performance and Fitness. Am Zool 23:347–361.

679 Barclay C.J. 2005. Modelling diffusive O_2 supply to isolated preparations of mammalian skeletal
680 and cardiac muscle. J Muscle Res Cell Motil 26:225–235.

Barclay C.J. 2023. A century of exercise physiology: key concepts in muscle energetics. Eur J Appl Physiol 123:25–42.

Barclay C.J., J.K. Constable, and C.L. Gibbs. 1993. Energetics of fast- and slow-twitch muscles of the mouse. J Physiol 472:61–80.

Bartholomew G.A. 1964. The roles of physiology and behavior in the maintenance of homeostasis in the desert environment. Symp Soc Exp Biol 18:7–29.

Bauwens D., T. Garland Jr., A.M. Castilla, and R.V. Damme. 1995. Evolution of sprint speed in Lacertid lizards: Morphological, physiological and behavioral covariation. Evolution 848–863.

Beck O.N., J. Gosyne, J.R. Franz, and G.S. Sawicki. 2020. Cyclically producing the same average muscle-tendon force with a smaller duty increases metabolic rate. Proc R Soc B Biol Sci 287:20200431.

Biewener A., R.McN. Alexander, and N.C. Heglund. 1981. Elastic energy storage in the hopping of kangaroo rats *(Dipodomys spectabilis)*. J Zool 195:369–383.

Biewener A.A. and T.J. Roberts. 2000. Muscle and tendon contributions to force, work and elastic energy savings: A comparative perspective. Exerc Sports Sci Rev 28:99–107.

Bonine K.E., T.T. Gleeson, and T. Garland Jr. 2005. Muscle fiber-type variation in lizards (*Squamata*) and phylogenetic reconstruction of hypothesized ancestral states. J Exp Biol 208:4529–4547.

699 Bottinelli R., Canepari M., Reggiani C. and Stienen G.J.M. 1994. Myofibrillar ATPase
700 consumption during isometric contraction and isomyosin composition in rat single skinned muscle
701 fibers. J Physiol 481:663-675

702 Bullimore S.R. and J.F. Burn. 2005. Scaling of elastic energy storage in mammalian limb tendons:
703 do small mammals really lose out? Biol Lett 1:57–59.

704 Cadney M.D., N.E. Schwartz, M.P. McNamara, M.P. Schmill, A.A. Castro, D.A. Hillis, and T.
705 Garland Jr. 2021. Cross-fostering selectively bred High Runner mice affects adult body mass but
706 not voluntary exercise. Physiol Behav 241:113569.

707 Careau V., M.E. Wolak, P.A. Carter, and T. Garland Jr. 2013. Limits to behavioral evolution: The
708 quantitative genetics of a complex trait under directional selection. Evolution 67:3102–3119.

709 Castro A.A., T. Garland Jr., S. Ahmed, and N.C. Holt. 2022. Trade-offs in muscle physiology in
710 selectively bred high runner mice. J Exp Biol 225:jeb244083.

711 Charles J.P., O. Cappellari, A.J. Spence, J.R. Hutchinson, and D.J. Wells. 2016. Musculoskeletal
712 geometry, muscle architecture and functional specializations of the mouse hindlimb. (W. D.
713 Phillips, ed.)PLOS ONE 11:e0147669.

714 Christensen B.A., D.C. Lin, M.J. Schwaner, and C.P. McGowan. 2022. Elastic energy storage
715 across speeds during steady-state hopping of desert kangaroo rats (*Dipodomys deserti*). J Exp Biol
716 225:jeb242954.

717 Claghorn G.C., Z. Thompson, J.C. Kay, G. Ordonez, T.G. Hampton, and T. Garland Jr. 2017.
718 Selective breeding and short-term access to a running wheel alter stride characteristics in house
719 mice. Physiol Biochem Zool 90:533–545.

720 Cook R.D. and W. Sanford. 1999. Applied regression including computing and graphics. John
721 Wiley & Sons, Inc., New York, NY.

722 Curry J.W., R. Hohl, T.D. Noakes, and T.A. Kohn. 2012. High oxidative capacity and type IIx
723 fibre content in springbok and fallow deer skeletal muscle suggest fast sprinters with a resistance
724 to fatigue. J Exp Biol 215:3997–4005.

725 Dlugosz E.M., M.A. Chappell, D.G. McGillivray, D.A. Syme, and T. Garland Jr. 2009.
726 Locomotor trade-offs in mice selectively bred for high voluntary wheel running. J Exp Biol
727 212:2612–2618.

728 Ettema G.J.C. 1996. Elastic and length–force characteristics of the gastrocnemius of the hopping
729 mouse (*Notomys Alexis*) and the rat (*Rattus Norvegicus*). J Exp Biol 199:1277–1285.

730 Fletcher J.R. and B.R. MacIntosh. 2017. Running economy from a muscle energetics perspective.
731 Front Physiol 8:433.

732 Foster C. and A. Lucia. 2007. Running economy: the forgotten factor in elite performance. Sports
733 Med 37:316–319.

734 Foster K.L., T. Garland Jr., L. Schmitz, and T.E. Higham. 2018. Skink ecomorphology: forelimb
735 and hind limb lengths, but not static stability, correlate with habitat use and demonstrate multiple
736 solutions. Biol J Linn Soc.

737 Garland Jr. T., M.T. Morgan, J.G. Swallow, J.S. Rhodes, I. Girard, J.G. Belter, and P.A. Carter.
738 2002. Evolution of a small-muscle polymorphism in lines of house mice selected for high activity
739 levels. Evolution 56:1267–1275.

740 Garland Jr. T. 1988. Genetic basis of activity metabolism I. Inheritance of speed, stamina, and
741 antipredator displays in the garter snake *Thamnophis sirtalis*. Evolution 42:335–350.

742 Garland Jr. T. 2003. Selection experiments: An under-utilized tool in biomechanics and
743 organismal biology. Vertebr Biomech Evol. Bios Scientific Publisher, Oxford.

744 Garland Jr. T. and P.A. Carter. 1994. Evolutionary Physiology. Annu Rev Physiol 56:579–621.

745 Garland Jr. T., C.J. Downs, and A.R. Ives. 2022. Trade-offs (and constraints) in organismal
746 biology. Physiol Biochem Zool 95:82–112.

747 Garland Jr. T. and P.L. Else. 1987. Seasonal, sexual, and individual variation in endurance and
748 activity metabolism in lizards. Am J Physiol-Regul Integr Comp Physiol 252:R439–R449.

749 Garland Jr. T. and C.M. Janis. 1993. Does metatarsal/femur ratio predict maximal running speed
750 in cursorial mammals? J Zool 229:133–151.

751 Garland Jr. T., S.A. Kelly, J.L. Malisch, E.M. Kolb, R.M. Hannon, B.K. Keeney, S.L. Van Cleave,
752 et al. 2011. How to run far: multiple solutions and sex-specific responses to selective breeding for
753 high voluntary activity levels. Proc R Soc B Biol Sci 278:574–581.

754 Garland Jr. T. and M.R. Rose. 2009. Experimental evolution: concepts, methods, and applications
755 of selection experiments. University of California Press, Berkeley.

Girard I., M.W. McAleer, J.S. Rhodes, and T. Garland Jr. 2001. Selection for high voluntary wheel-running increases speed and intermittency in house mice (*Mus domesticus*). J Exp Biol 204:4311–4320.

Gleeson T.T. and J.M. Harrison. 1988. Muscle composition and its relation to sprint running in the lizard *Dipsosaurus dorsalis*. Am J Physiol-Regul Integr Comp Physiol 255:R470–R477.

Green H., H. Reichmann, and D. Pette. 1983. Fiber type specific transformations in the enzyme activity pattern of rat vastus lateralis muscle by prolonged endurance training. Pflugers Arch 399:216–222.

Guderley H., Houle-Leroy P., G.M. Diffee, D.M. Camp, and T. Garland Jr. 2006. Morphometry, ultrastructure, myosin isoforms, and metabolic capacities of the "mini muscles" favoured by selection for high activity in house mice. Comp Biochem Physiol B Biochem Mol Biol 144:271–282.

He Z.H., R. Bottinelli, M.A. Pellegrino, M.A. Ferenczi, and C. Reggiani. 2000. ATP consumption and efficiency of human single muscle fibers with different myosin isoform composition. Biophys J 79:945–961.

Heglund N.C., M.A. Fedak, C.R. Taylor, and G.A. Cavagna. 1982. Energetics and mechanics of terrestrial locomotion. IV Total mechanical energy changes as a function of speed and body size in birds and mammals. J Exp Biol 97:57–66.

Hill A.V. 1951. The effect of series compliance on the tension developed in a muscle twitch. Proc R Soc Lond B Biol Sci 138:325–329.

776 Hiramatsu L., J.C. Kay, Z. Thompson, J.M. Singleton, G.C. Claghorn, R.L. Albuquerque, B. Ho,
777 et al. 2017. Maternal exposure to Western diet affects adult body composition and voluntary wheel
778 running in a genotype-specific manner in mice. Physiol Behav 179:235–245.

779 Holt N.C. 2019. Beyond bouncy gaits: The role of multiscale compliance in skeletal muscle
780 performance. J Exp Zool Part Ecol Integr Physiol 333:50–59.

781 Holt N.C., N. Danos, T.J. Roberts, and E. Azizi. 2016. Stuck in gear: age-related loss of variable
782 gearing in skeletal muscle. J Exp Biol 219:998–1003.

783 Holt N.C. and D.L. Mayfield. 2023. Muscle-tendon unit design and tuning for power
784 enhancement, power attenuation, and reduction of metabolic cost. J Biomech 153:111585.

785 Holt N.C., T.J. Roberts, and G.N. Askew. 2014. The energetic benefits of tendon springs in
786 running: is the reduction of muscle work important? J Exp Biol jeb.112813.

787 Hoogkamer W., S. Kipp, B.A. Spiering, and R. Kram. 2016. Altered running economy directly
788 translates to altered distance-running performance. Med Sci Sports Exerc 48:2175–2180.

789 Houle-Leroy P., T. Garland Jr., Swallow J.G., and Guderley H. 2000. Effects of voluntary activity
790 and genetic selection on muscle metabolic capacities in house mice *Mus domesticus*. J Appl
791 Physiol 89:1608–1616.

792 Houle-Leroy P., H. Guderley, J.G. Swallow, and T. Garland Jr. 2003. Artificial selection for high
793 activity favors mighty mini-muscles in house mice. Am J Physiol-Regul Integr Comp Physiol
794 284:R433–R443.

795 Huey R.B. and A.F. Bennett. 1987. Phylogenetic studies of coadaptation: Preferred temperatures
796 versus optimal performance temperatures of lizards. Evolution 41:1098–1115.

797 Husak J.F. 2006. Does speed help you survive? A test with Collared Lizards of different ages.
798 Funct Ecol 20:174–179.

799 Jenkins F.A. and S.M. Camazine. 1977. Hip structure and locomotion in ambulatory and cursorial
800 carnivores. J Zool 181:351–370.

801 Josephson R.K., J.G. Malamud, and D.R. Stokes. 2000. Asynchronous muscle: A primer. J Exp
802 Biol 203:2713–2722.

803 Joyner M.J. and E.F. Coyle. 2008. Endurance exercise performance: the physiology of champions:
804 factors that make champions. J Physiol 586:35–44.

805 Khan, R. H., J. S. Rhodes, I. A. Girard, N. E. Schwartz, and T. Garland, Jr. 2024. Does behavior
806 evolve first? Correlated responses to selection for voluntary wheel-running behavior in house
807 mice. Ecological and Evolutionary Physiology 97:In press.

808 Kohn T.A. 2014. Insights into the skeletal muscle characteristics of three southern African
809 antelope species. Biol Open 3:1037–1044.

810 Kohn T.A., R. Burroughs, M.J. Hartman, and T.D. Noakes. 2011. Fiber type and metabolic
811 characteristics of lion (*Panthera leo*), caracal (*Caracal caracal*) and human skeletal muscle. Comp
812 Biochem Physiol A Mol Integr Physiol 159:125–133.

813 Kolb E.M., S.A. Kelly, K.M. Middleton, L.S. Sermsakdi, M.A. Chappell, and T. Garland Jr. 2010.
814 Erythropoietin elevates but not voluntary wheel running in mice. J Exp Biol 213:510–519.

Kram R. and C.R. Taylor. 1990. Energetics of running: a new perspective. Nature 346:265–267.

Labonte D. 2023. A theory of physiological similarity in muscle-driven motion. PNAS 120:e2221217120.

Labonte D. and N.C. Holt. 2022. Elastic energy storage and the efficiency of movement. Curr Biol 32:R661–R666.

Lappin A.K. and J.F. Husak. 2005. Weapon performance, not size, determines mating success and potential reproductive output in the Collard lizard (*Crotaphytus collaris*). Am Nat 166:426–436.

Lerman I., B.C. Harrison, K. Freeman, T.E. Hewett, D.L. Allen, J. Robbins, and L.A. Leinwand. 2002. Genetic variability in forced and voluntary endurance exercise performance in seven inbred mouse strains. J Appl Physiol 92.

Lindstedt S.L., T. McGlothlin, E. Percy, and Pifer, J. 1998. Task-specific design of skeletal muscle: balancing muscle structural composition. Comp Biochem Physiol 120:35–40.

Mayfield D.L., B.S. Launikonis, A.G. Cresswell, and G.A. Lichtwark. 2016. Additional in-series compliance reduces muscle force summation and alters the time course of force relaxation during fixed-end contractions. J Exp Biol 219:3587–3596.

Mayr E. 1963. Animal species and evolution. Harvard University Press, Cambridge, MA.

McGillivray D.G., T. Garland Jr., Dlugosz E.M., Chappell M.A., and Syme D.A. 2009. Changes in efficiency and myosin expression in the small-muscle phenotype of mice selectively bred for high voluntary running activity. J Exp Biol 212:977–985.

834 Mendez J, and Keys A. 1960. Density and composition of mammalian muscle. Met Clin Exp
835 9:184-188
836 Mendoza E. and Azizi E. 2021. Tuned muscle and spring properties increase elastic energy
837 storage. J Exp Biol 224:jeb243180.

838 Moen D.S. 2019. What determines the distinct morphology of species with a particular ecology?
839 The roles of many-to-one mapping and trade-offs in the evolution of frog ecomorphology and
840 performance. Am Nat 194:E81–E95.

841 Morgan T.J., M.A. Evans, T. Garland Jr., J.G. Swallow, and P.A. Carter. 2005. Molecular and
842 quantitative genetic divergence among populations of house mice with known evolutionary
843 histories. Heredity 94:518–525.

844 Myers M.J. and K. Steudel. 1985. Effect of limb mass and its distribution on the energetic cost of
845 running. J Exp Biol 116:363–373.

846 Picasso M.B.J. 2010. The Hindlimb Muscles of Rhea americana (*Aves, Palaeognathae, Rheidae*):
847 Pelvic Limb Muscles of Rhea. Anat Histol Embryol 462–472.

848 Pollock C.M. and R.E. Shadwick. 1994. Allometry of muscle, tendon, and elastic energy storage
849 capacity in mammals. Am J Physiol-Regul Integr Comp Physiol 266:R1022–R1031.

850 Powell P.L., R.R. Roy, P. Kanim, M.A. Bello, and V.R. Edgerton. 1984. Predictability of skeletal
851 muscle tension from architectural determinations in guinea pig hindlimbs. J Appl Physiol
852 57:1715–1721.

Rezende E.L., F.R. Gomes, M.A. Chappell, and T. Garland Jr. 2009. Running behavior and its energy cost in mice selectively bred for high voluntary locomotor activity. Physiol Biochem Zool 82:662–679.

Rivero J.L., A.L. Serrano, P. Henckel, and E. Aguera. 1993. Muscle fiber type compositon and fiber size in successfully and unsucessfully endurance-raced horses. J Appl Physiol 75:1758–1766.

Rivero J.L.L., R.J. Talmadge, and V.R. Edgerton. 1999. Interrelationships of myofibrillar ATPase activity and metabolic properties of myosin heavy chain-based fibre types in rat skeletal muscle. Histochem Cell Biol 111:277–287.

Roberts T.J., R. Kram, P.G. Weyand, and C.R. Taylor. 1998. Energetics of bipedal running: I. metabolic cost of generating force. J Exp Biol 201:2745–2751.

Roberts T.J., R.L. Marsh, P.G. Weyand, and C.R. Taylor. 1997. Muscular force in running turkeys: the economy of minimizing work. Science 275:1113–1115.

Roff D.A. and D.J. Fairbairn. 2007. The evolution of trade-offs: where are we? J Evol Biol 20:433–447.

Rome L.C., D.A. Syme, S. Hollingworth, S.L. Lindstedt, and S.M. Baylor. 1996. The whistle and the rattle: the design of sound producing muscles. Proc Natl Acad Sci 93:8095–8100.

Rubenson J., D.G. Lloyd, D.B. Heliams, T.F. Besier, and P.A. Fournier. 2011. Adaptations for economical bipedal running: the effect of limb structure on three-dimensional joint mechanics. J R Soc Interface 8:740–755.

872 Scales J.A. and M.A. Butler. 2016. Adaptive evolution in locomotor performance: how selective
873 pressures and functional relationships produce diversity. Evolution 70:48–61.

874 Schiaffino S. and C. Reggiani. 2011. Fiber types in mammalian skeletal muscles. Physiol Rev
875 91:1447–1531.

876 Schwartz N.E., M.P. McNamara, J.M. Orozco, J.O. Rashid, A.P. Thai, and Garland, Jr. 2023.
877 Selective breeding for high voluntary exercise in mice increases maximal VO2max but not basal
878 metabolic rate. J Exp Biol 226:jeb245256.

879 Shoval O., H. Sheftel, G. Shinar, Y. Hart, O. Ramote, A. Mayo, E. Dekel, et al. 2012.
880 Evolutionary trade-offs, pareto optimality, and the geometry of phenotypic space. Science
881 336:1157–1160.

882 Swallow J.G., P.A. Carter, and T. Garland Jr. 1998. Artificial selection for increased wheel-
883 running behavior in house mice. Behav Genet 28:227–237.

884 Syme D.A., K. Evashuk, B. Grintuch, E.L. Rezende, and T. Garland Jr. 2005. Contractile abilities
885 of normal and "mini" triceps surae muscles from mice (*Mus domesticus*) selectively bred for high
886 voluntary wheel running. J Appl Physiol 99:1308–1316.

887 Talmadge R.J., W. Acosta, and T. Garland Jr. 2014. Myosin heavy chain isoform expression in
888 adult and juvenile mini-muscle mice bred for high-voluntary wheel running. Mech Dev 134:16–
889 30.

890 Trappe S., M. Harber, A. Creer, P. Gallagher, D. Slivka, K. Minchev, and D. Whitsett. 2006.
891 Single muscle fiber adaptations with marathon training. J Appl Physiol 101:721–727.

892 Wainwright P.C., E. Alfaro, D.I. Bolnick, and C.D. Hulsey. 2005. Many-to-one mapping of form
893 to function: a general principle in organismal design? Integr Comp Biol 45:256–262.

894 Waters R.P., K.J. Renner, R.B. Pringle, C.H. Summers, S.L. Britton, L.G. Koch, and J.G.
895 Swallow. 2008. Selection for aerobic capacity affects corticosterone, monoamines and wheel-
896 running activity. Physiol Behav 93:1044–1054.

897 Williams C.D. and N.C. Holt. 2018. Spatial scale and structural heterogeneity in skeletal muscle
898 performance. Integr Comp Biol 58:163–173.

899 Wilson A. and G. Lichtwark. 2011. The anatomical arrangement of muscle and tendon enhances
900 limb versatility and locomotor performance. Philos Trans R Soc B Biol Sci 366:1540–1553.

901 Wilson R.S., R.S. James, and R.V. Damme. 2002. Trade-offs between speed and endurance in the
902 frog Xenopus laevis: a multi-level approach. J Exp Biol 205:1145–1152.

903 Young D. and R.K. Josephson. 1983. Mechanisms of sound-production and muscle contraction
904 kinetics in cicadas. J Comp Physiol A 152:183–195.

905

906

907 **Figure legends**

908

909 Fig. 1 – Triceps surae muscle mass (A) and muscle-tendon unit length (B) as a function of body
910 mass for all eight lines, with individuals from HR line 6 separated into mini-muscle (HR6M) vs
911 normal-muscle (HR6N) individuals. In A, mice from HR lines have reduced muscle mass and mini-
912 muscle individuals have even lighter muscles, with a positive effect of body mass (for log-log
913 transformed data, the allometric scaling exponent from the statistical model = 0.846 with a standard
914 error of 0.180). In B, MTU length is unaffected by linetype or mini-muscle status, but body mass
915 had a positive effect of body mass (for log-log transformed data, the allometric scaling exponent =
916 0.243 with a standard error of 0.102).

917

918 Fig. 2 – Triceps surae muscle belly length (A) and Achilles tendon (B) length as a function of body
919 mass for all lines, with individuals from HR line 6 separated into mini-muscle (HR6M) vs normal-
920 muscle (HR6N) individuals. Mice from the HR lines have shorter muscles and longer tendons. For
921 log-log transformed data, the allometric scaling exponents from the statistical models are 0.255 +
922 0.145 (SE) for muscle belly length and 0.330 + 0.278 for tendon length.

923

924 Fig. 3 – Twitch rise (TP_{tw}) and half relaxation (TP_{50}) for all HR (solid bars), highlighting HRnorm
925 (black) and HRmini (grey) lines, and C (open bars) lines. Least squares means and standard errors
926 show that, for both traits, values for HR mice are significantly reduced when compared with C lines.

927

928 Fig. 4 – (A) Relationship between resistive force and absolute shortening velocity for values from
929 all individual mice. Data were analyzed as repeated-measures models in SAS Procedure MIXED.

See text for explanation of results. Age was also included as a covariate (not shown). (B) V_{max} values obtained from the extrapolation of second order polynomial fits to the force-velocity data to zero force for each individual mouse, as shown in A, then compared among nine "lines" (also in SAS Procedure MIXED, but "line" was treated as a fixed effect). Least squares means and standard errors show that V_{max} values are lower in HRmini (grey bars: HR3M, HR6M) than HRnorm lines or individuals, with some variation observed across C (open bars: C1, C2, C4, C5) and HRnorm lines (black bars: HR6N, HR7, HR8).

Fig. 5 – (A) Relationship between resistive force and normalized shortening velocity for values from all individual mice. Data were analyzed as repeated-measures models in SAS Procedure MIXED. See text for explanation of results. Age was also included as a covariate (not shown). (B) $V_{normmax}$ values obtained from the extrapolation of second order polynomial fits to the force-velocity data to zero force for each individual mouse, as shown in A, then compared among nine "lines" (also in SAS Procedure MIXED, but "line" was treated as a fixed effect). Least squares means and standard errors show that $V_{normmax}$ values are both higher and lower in HR mice than C mice, with HRmini lines/individuals (grey bars) having the lowest values, and there being considerable variation across HRnorm lines (black bars).

Fig. 6 – Least squares means and standard errors from analyses comparing the nine "lines" for $Endur_{0\text{-}90}$ (A) and Sustained F/F_0 (B) metrics. ANOVA tables are from comparisons of HR with C lines and normal with mini-muscle individuals (SAS Procedure Mixed). Least squares means and standard errors show that $Endur_{0\text{-}90}$ declines much more slowly in HRmini individuals (grey bars: HR3M, HR6M) than in HRnorm lines or individuals, and HRnorm mice have a slower decline than

953 do C mice, with some variation observed across C (open bars: C1, C2, C4, C5) and across HRnorm
954 lines (black bars: HR6N, HR7, HR8). Least squares means and standard errors also show that
955 Sustained F/F_0 is much higher in mini-muscle individuals than in normal-muscle individuals, with
956 no difference between HRnorm and C mice. (C-F) Sample endurance traces from individuals for
957 four lines, HRmini (C), HRnorm (D), and C (E, F).
958
959 Fig. 7 – Relationship between velocity (V_{max}) and endurance ($Endur_{0\text{-}90}$) metrics across HR (solid
960 symbols) and C (open symbols) lines, highlighting HRmini (black) and HRnoRM (grey) lines or
961 individuals. The correlation for the C lines is 0.868, which differs significantly (2-tailed p=0.0031)
962 from the correlation for the five HR "lines (r=-0.980). Additional scatterplots and analyses are found
963 in Supplemental Figure S2 and discussed in the Results section.
964
965

966 Figure 1

967

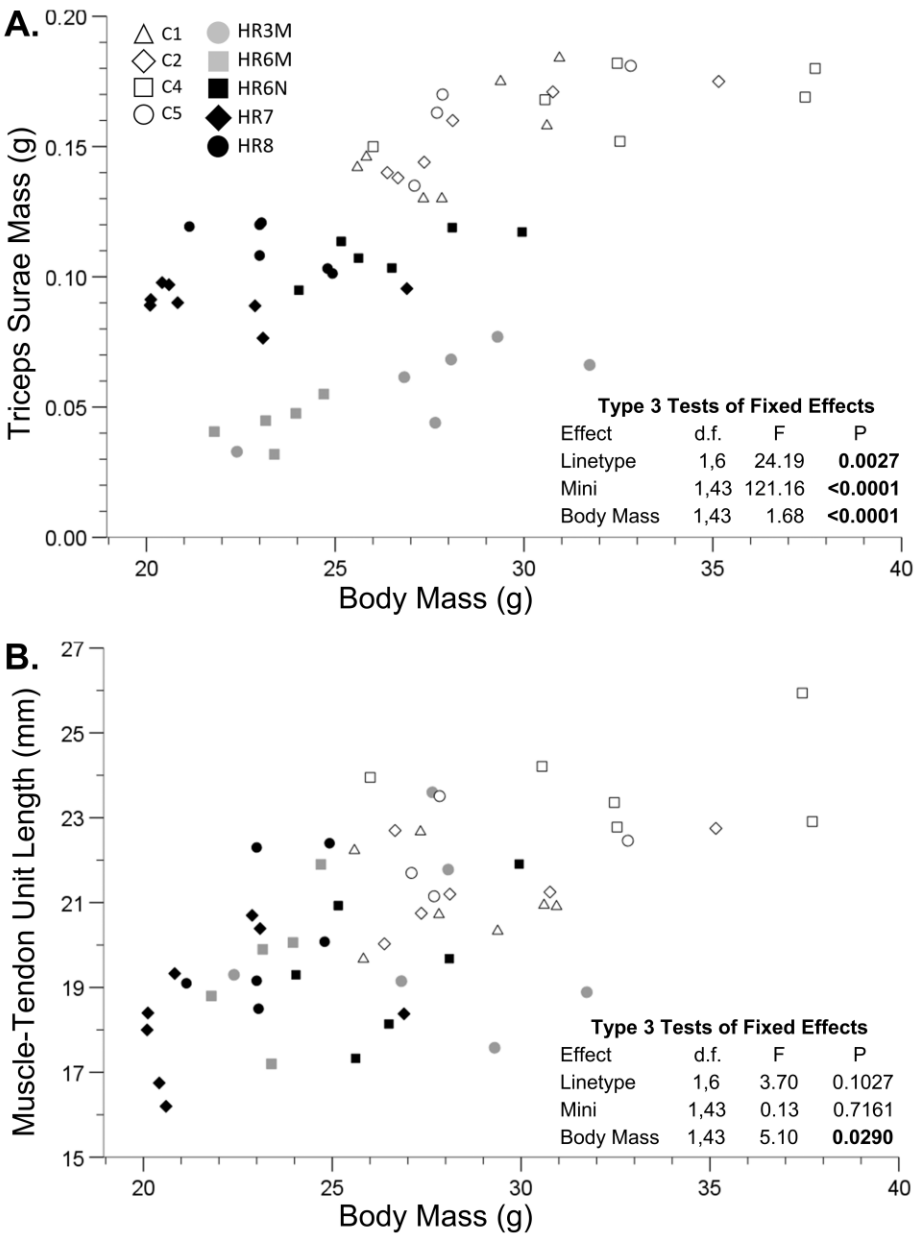

968

969

970 Figure 2

971

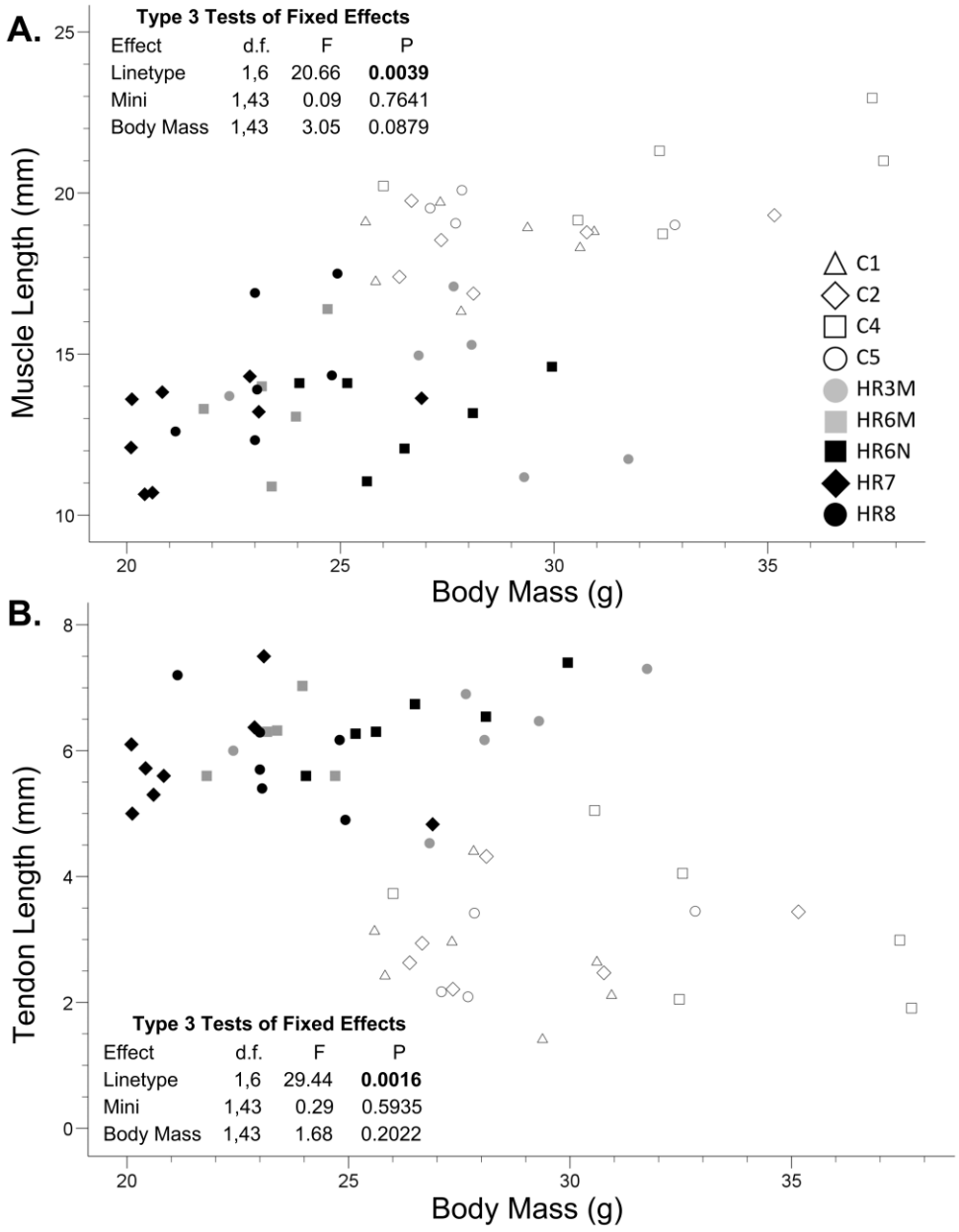

972

973

974

975 Figure 3

976

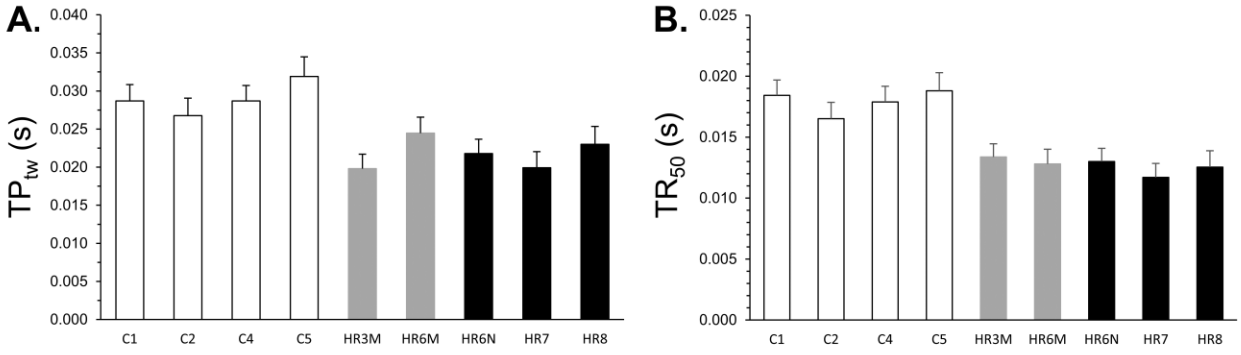

Type 3 Tests of Fixed Effects

Effect	d.f.	F	P
Linetype	1,6	8.20	**0.0286**
Mini	1,43	0.15	0.7016

Type 3 Tests of Fixed Effects

Effect	d.f.	F	P
Linetype	1,6	12.76	**0.0118**
Mini	1,43	0.58	0.4489

977

978

979

980 Figure 4

981

982

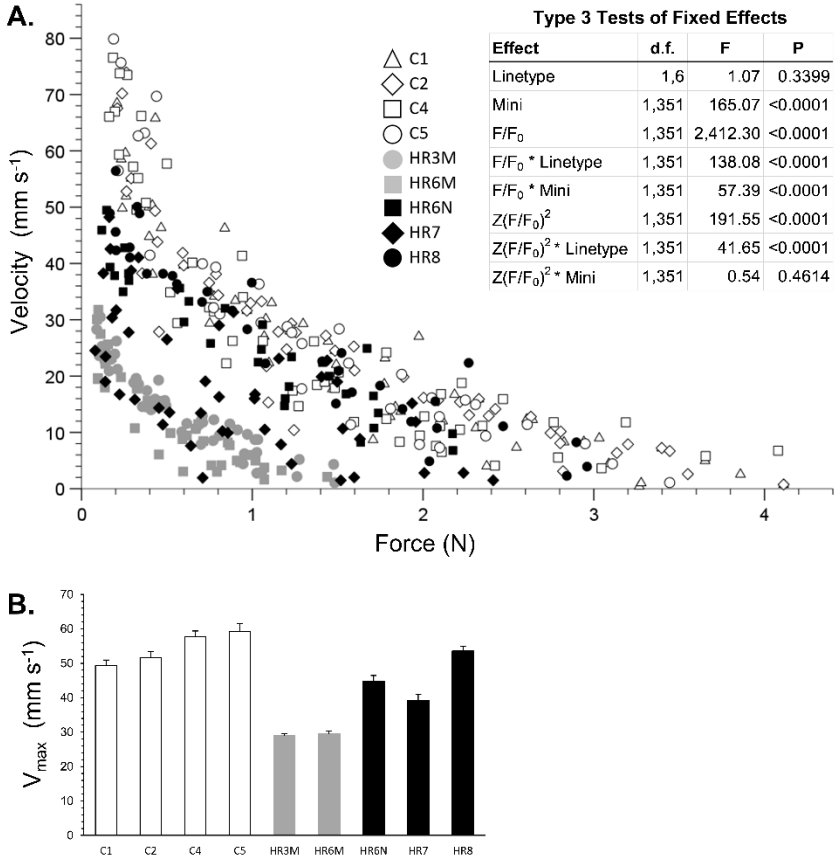

983

984

985

986 Figure 5

987

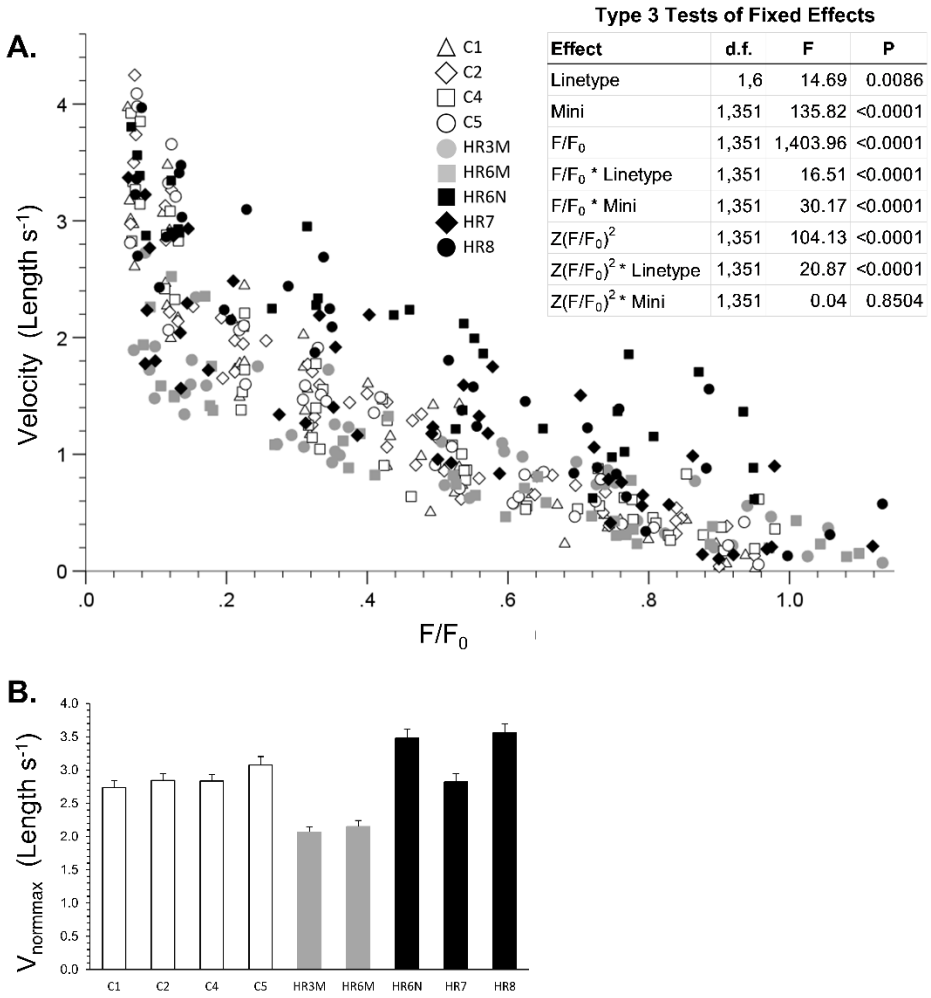

Type 3 Tests of Fixed Effects

Effect	d.f.	F	P
Linetype	1,6	14.69	0.0086
Mini	1,351	135.82	<0.0001
F/F_0	1,351	1,403.96	<0.0001
F/F_0 * Linetype	1,351	16.51	<0.0001
F/F_0 * Mini	1,351	30.17	<0.0001
$Z(F/F_0)^2$	1,351	104.13	<0.0001
$Z(F/F_0)^2$ * Linetype	1,351	20.87	<0.0001
$Z(F/F_0)^2$ * Mini	1,351	0.04	0.8504

988

989

990

991

992

993

994

Figure 6

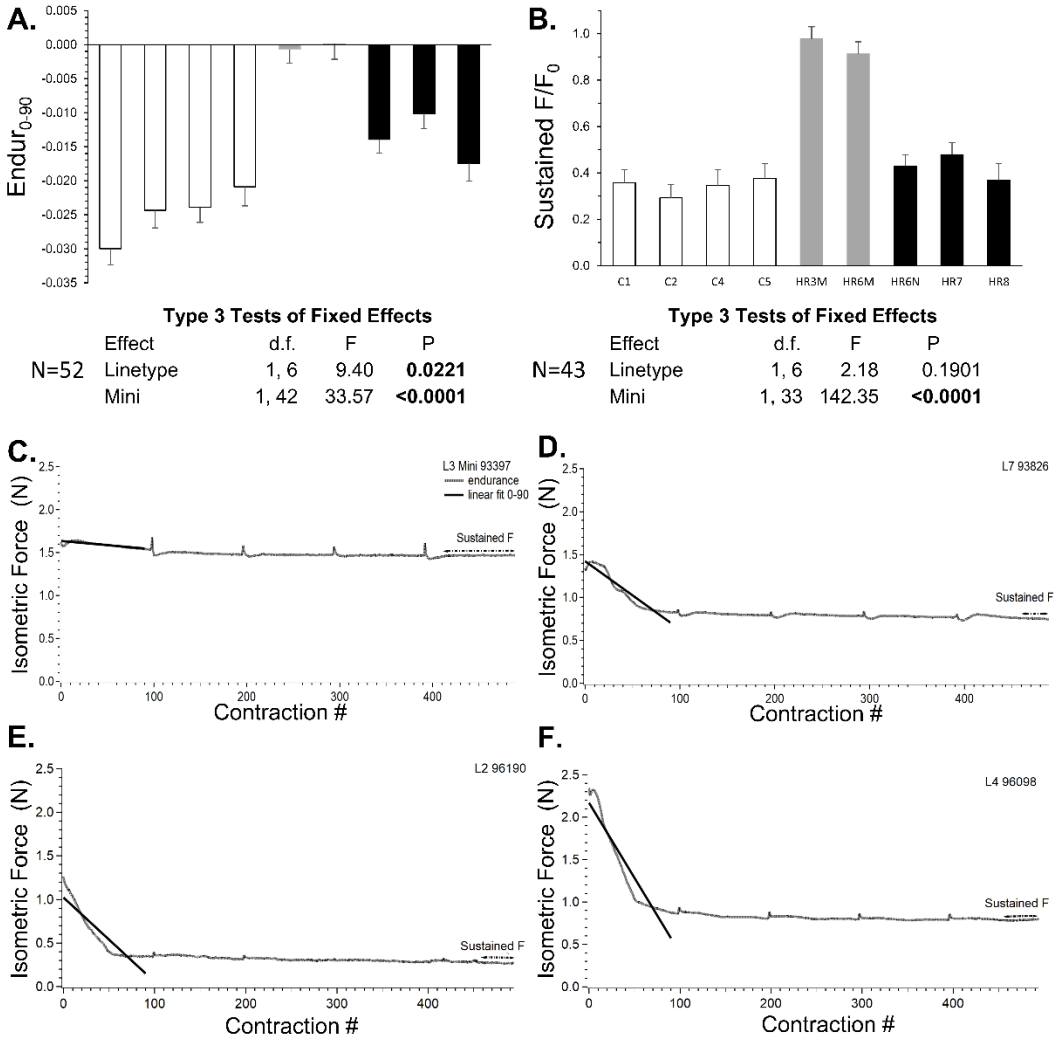
A.
Endur0-90
B.
Sustained F/F0
C1
C2
C4
C5
HR3M
HR6M
HR6N
HR7
HR8
Type 3 Tests of Fixed Effects
Effect d.f. F P
N=52 Linetype 1, 6 9.40 0.0221
Mini 1, 42 33.57 <0.0001
Type 3 Tests of Fixed Effects
Effect d.f. F P
N=43 Linetype 1, 6 2.18 0.1901
Mini 1, 33 142.35 <0.0001
C.
L3 Mini 93397
endurance
linear fit 0-90
Sustained F
Isometric Force (N)
Contraction #
D.
L7 93826
Sustained F
Isometric Force (N)
Contraction #
E.
L2 96190
Sustained F
Isometric Force (N)
Contraction #
F.
L4 96098
Sustained F
Isometric Force (N)
Contraction #

1002 Figure 7

1003

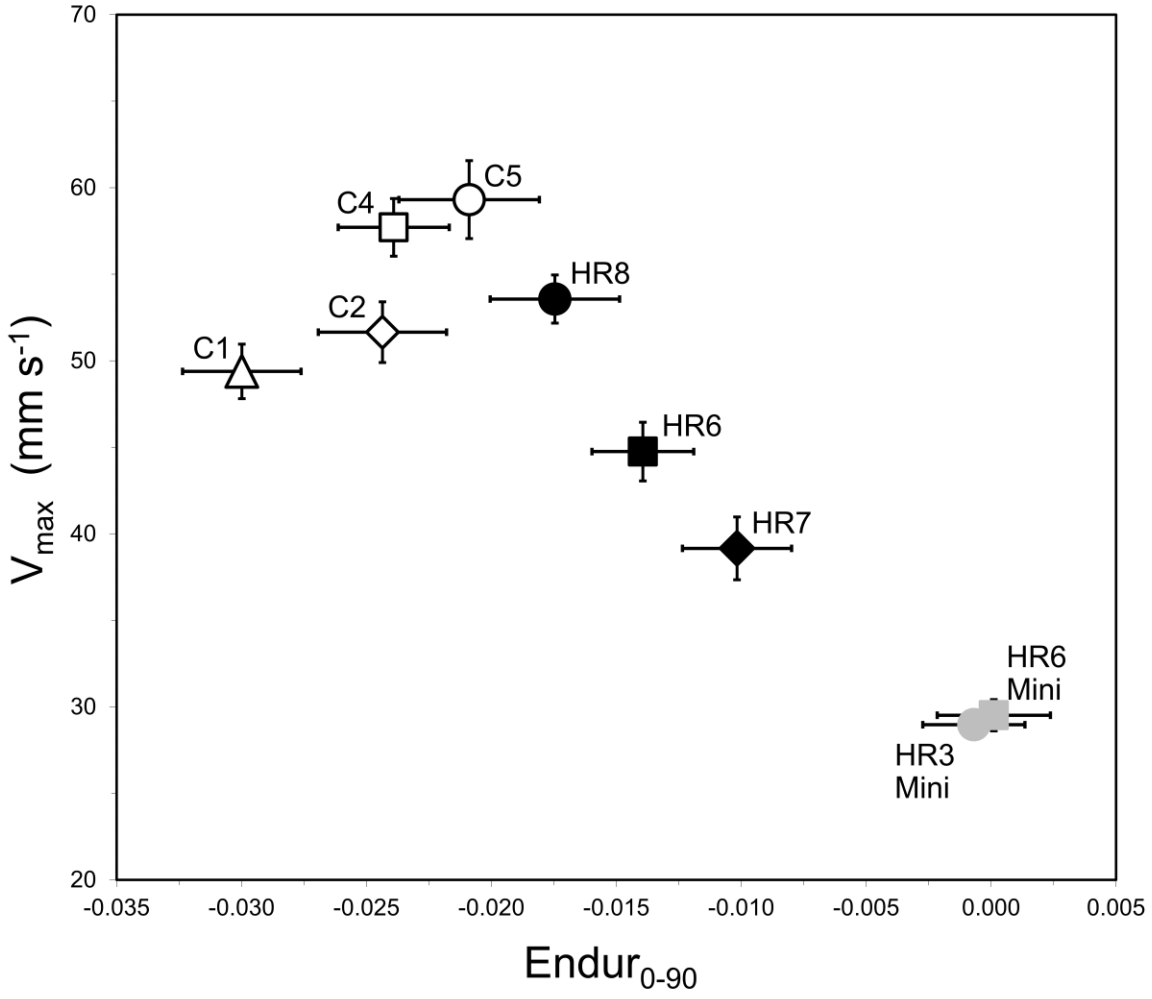

1004

1005

1006

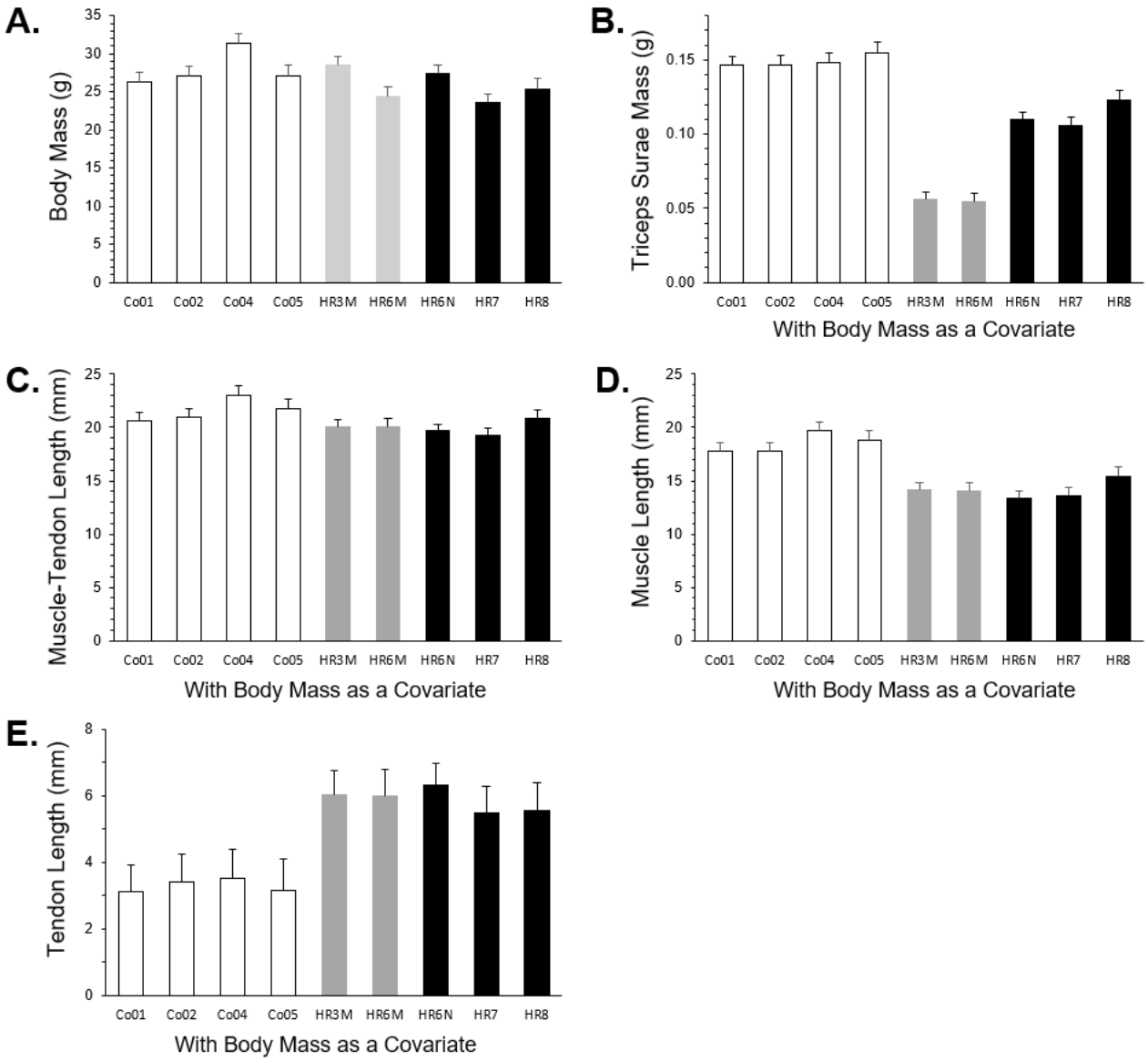

Supplemental Figure S1. Variation among the nine "lines" showing line HR6 separated into individuals with (HR6M) and without (HR6N) the mini-muscle phenotype. Values are Least Squares Means and Standard Errors from one-way ANCOVAs comparing the nine groups in SAS Procedure Mixed, with body mass and age as covariates (for analysis of body mass, only age was a covariate). Non-selected control (C) lines are in open bars, mini-muscle lines or individuals (for line HR6N) are in gray bars, and HR lines that are purely composed of normal-muscle individuals are in black bars. Of particular interest in these analyses was whether a trait varied significantly among the replicate C lines (which would indicate random mutation and/or genetic drift) or among the replicate HR lines (which may also indicate multiple adaptive responses to selection a.k.a. "multiple solutions"). Of particular note, the relative mass of the triceps surae muscle varied significantly among the three normal-muscled HR lines: muscle mass was larger in HR8 than HR7 (p=0.0114: differences of least squares means from SAS Procedure

Mixed), with values for HR6N being intermediate to them. For other examples of trait variation among the HR lines, see Figures 4, 5, and 6.

A.

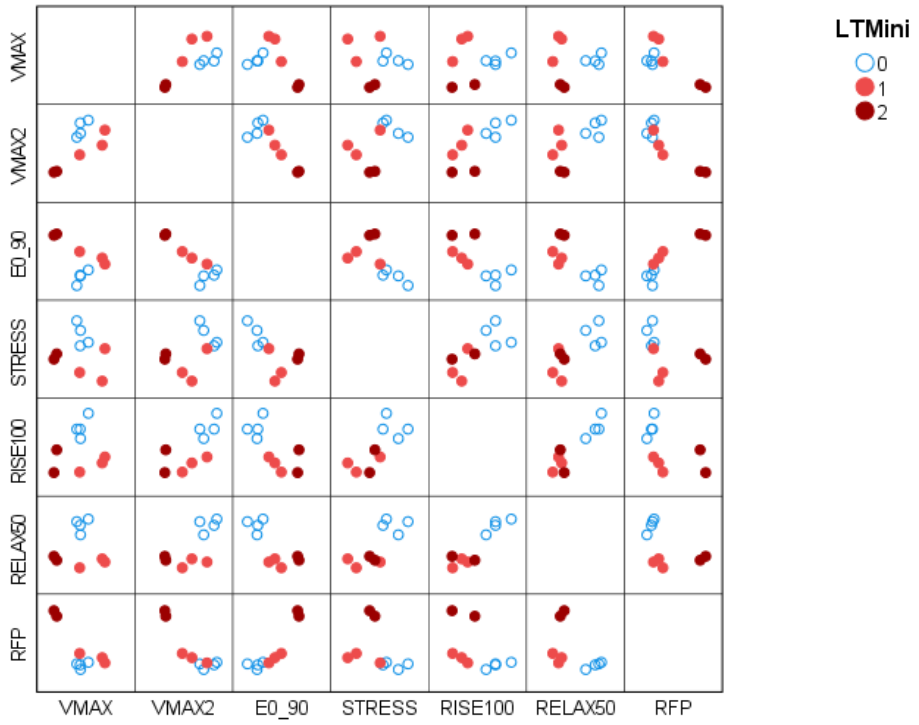

B.

Control (N=4)		VMAX	VMAX2	E0_90	STRESS	RISE100	RELAX50	RFP
VMAX	Pearson Correlation	1	0.798	0.891	-0.641	0.767	0.344	0.389
	Sig. (2-tailed)		0.2017	0.1093	0.3591	0.2329	0.6557	0.6112
VMAX2	Pearson Correlation	0.798	1	0.868	-0.954	0.689	0.388	0.466
	Sig. (2-tailed)	0.2017		0.1319	0.0457	0.3108	0.6122	0.5336
E0_90	Pearson Correlation	0.891	0.868	1	-0.845	0.482	0.013	0.084
	Sig. (2-tailed)	0.1093	0.1319		0.1550	0.5177	0.9871	0.9155
STRESS	Pearson Correlation	-0.641	-0.954	-0.845	1	-0.446	-0.155	-0.244
	Sig. (2-tailed)	0.3591	0.0457	0.1550		0.5539	0.8453	0.7563
RISE100	Pearson Correlation	0.767	0.689	0.482	-0.446	1	0.866	0.887
	Sig. (2-tailed)	0.2329	0.3108	0.5177	0.5539		0.1336	0.1129
RELAX50	Pearson Correlation	0.344	0.388	0.013	-0.155	0.866	1	0.996
	Sig. (2-tailed)	0.6557	0.6122	0.9871	0.8453	0.1336		0.0042
RFP	Pearson Correlation	0.389	0.466	0.084	-0.244	0.887	0.996	1
	Sig. (2-tailed)	0.6112	0.5336	0.9155	0.7563	0.1129	0.0042	

C.

Selected (N=5)		VMAX	VMAX2	E0_90	STRESS	RISE100	RELAX50	RFP
VMAX	Pearson Correlation	1	0.965	-0.983	-0.272	0.104	-0.278	-0.954
	Sig. (2-tailed)		0.0077	0.0027	0.6576	0.8682	0.6503	0.0119
VMAX2	Pearson Correlation	0.965	1	-0.980	-0.038	0.141	-0.322	-0.927
	Sig. (2-tailed)	0.0077		0.0033	0.9514	0.8206	0.5978	0.0232
E0_90	Pearson Correlation	-0.983	-0.980	1	0.223	-0.002	0.384	0.974
	Sig. (2-tailed)	0.0027	0.0033		0.7189	0.9971	0.5239	0.0051
STRESS	Pearson Correlation	-0.272	-0.038	0.223	1	0.484	0.155	0.337
	Sig. (2-tailed)	0.6576	0.9514	0.7189		0.4087	0.8034	0.5787
RISE100	Pearson Correlation	0.104	0.141	-0.002	0.484	1	0.122	0.016
	Sig. (2-tailed)	0.8682	0.8206	0.9971	0.4087		0.8446	0.9800
RELAX50	Pearson Correlation	-0.278	-0.322	0.384	0.155	0.122	1	0.546
	Sig. (2-tailed)	0.6503	0.5978	0.5239	0.8034	0.8446		0.3413
RFP	Pearson Correlation	-0.954	-0.927	0.974	0.337	0.016	0.546	1
	Sig. (2-tailed)	0.0119	0.0232	0.0051	0.5787	0.9800	0.3413	

D.

P-values for Difference of Correlation Coefficients

	VMAX2	E0_90	STRESS	RISE10(	RELAX5(	RFP
VMAX	0.4521	0.0019	0.6946	0.4582	0.5989	0.0621
VMAX2		0.0031	0.1337	0.5654	0.5439	0.0804
E0_90			0.2316	0.6666	0.7491	0.0893
STRESS				0.4105	0.7986	0.6244
RISE100					0.3295	0.2558
RELAX50						0.0417

E.

	Principal Component						
Variable	1	2	3	4	5	6	7
VMAX	.507	-.834	.039	.172	.108	-.069	.011
VMAX2	.937	-.262	.129	.072	-.018	.176	-.015
E0_90	-.959	.081	.202	.162	-.047	.047	.045
STRESS	.686	.595	-.368	.197	.015	.014	.014
RISE100	.847	.398	.303	.126	-.086	-.098	-.015
RELAX50	.840	.467	.192	-.160	.114	.011	.031
RFP	-.861	.454	.129	.124	.135	.023	-.033
Eigenvalue	4.69	1.71	4.86	2.24	0.05	0.05	0.01
% Variance	67.0	24.3	4.9	2.2	0.8	0.7	0.1
Cumulative %	67.0	91.4	96.2	98.5	99.2	99.9	100.0

F.

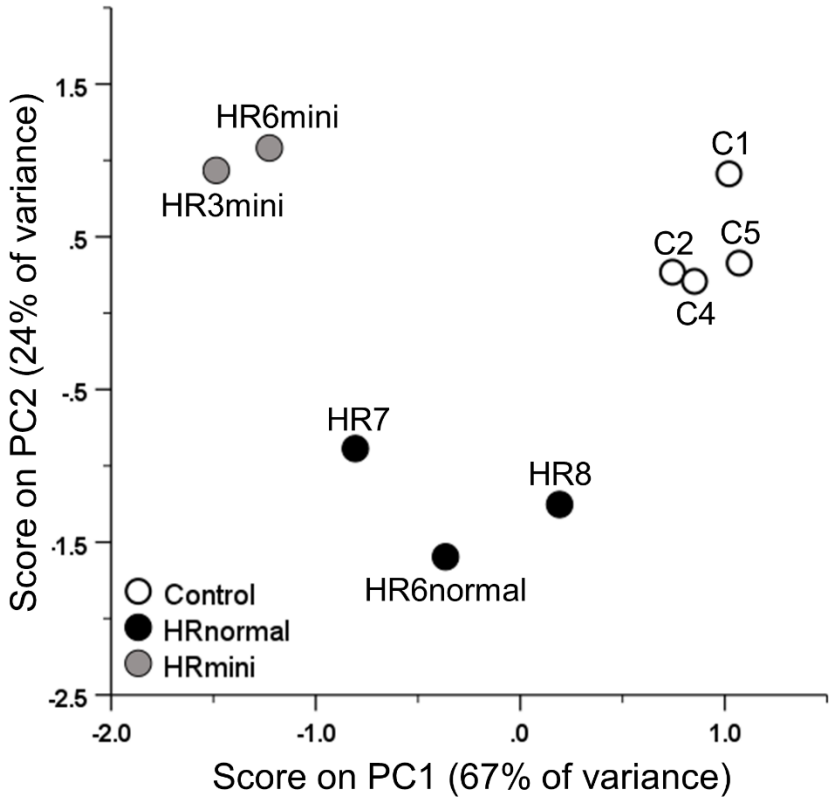

Supplemental Figure S2. Analyses of correlations using least squares means for nine "lines" (line HR6 separated into individuals with without the mini-muscle phenotype) from one-way ANCOVAs comparing the nine groups in SAS Procedure Mixed. A) Bivariate scatterplots. B) Pearson correlations and 2-tailed significance for the four C lines. C) Pearson correlations and 2-tailed significance for the five HR "lines. D) Tests for difference between the C and HR correlation coefficients. E) Factor loadings (component correlations) of each variable with each of the seven principal components (PCs), based on analysis of the correlation matrix for all seven muscle contractile traits. F) Scatterplot of scores on the first two principal components, which together account for 91.4% of the total variation in contractile properties among the nine "line" means. Note that due to space and notation constraints different abbreviations are used here compared to the main manuscript (VMAX = $V_{normmax}$, VMAX2 = V_{max}, $E_{0\text{-}90}$ = $Endur_{0\text{-}90}$, RFP = Sustained F/F_0, RISE100 = TP_{tw} , RELAX50 = TR_{50}).